1992A&A...254..436B

Astron. Astrophys. 254, 436–453 (1992)

ASTRONOMY AND ASTROPHYSICS

On the analysis of collision strengths and rate coefficients

A. Burgess[1] **and J. A. Tully**[2]

[1] Department of Applied Mathematics and Theoretical Physics, Silver Street, Cambridge CB3 9EW, England, UK
[2] Observatoire de la Côte d'Azur, CNRS (URA 1362), BP 139, F-06003 Nice Cedex, France

Received December 20, 1990; accepted June 19, 1991

Abstract. This paper presents a new way of critically assessing and compacting data for electron impact excitation of positive ions. Collision strengths Ω are scaled and then plotted as functions of the colliding electron energy, the complete range of energies being mapped onto the interval (0, 1). The scaled Ω can then be represented to good accuracy by a 5-point spline. Similar scaling and spline fitting techniques enable thermally averaged collision strengths Y to be obtained at all temperatures. Whole isoelectronic sequences may then be treated by mapping the ion charge onto (0, 1) and using a second 5-point spline; thus reducing Y, for the whole sequence and all temperatures, to a 5×5 array. Three main types of transition (optically allowed, forbidden and exchange) are discussed separately and illustrated by numerical examples. Interactive programs for analysing atomic data in this way have been developed.

Key words: excitation rate coefficient – positive ions – spectroscopy – corona – data compaction

1. Introduction

Accurate atomic data, required in the analysis of astrophysical and laboratory plasmas, is becoming available in rapidly increasing amounts from many diverse sources, experimental and theoretical. For this reason, and because increasing complexity of calculation may lead to increasing chance of systematic and random error, there is need for simple methods to check and compare data on a uniform basis. For the user, this mass of data then needs to be made available in as simple and compact a form as possible, consistent with no significant reduction in accuracy.

Many attempts have been made to parametrise rate coefficients as functions of temperature T. Extensive use has been made, for example, of the fits given by Mewe (1972). Many other similar fitting formulae which reproduce approximately the results of collision calculations have been proposed. Of particular interest is the 9-parameter expression based on distorted wave calculations by Clark et al. (1982). We ought also to mention the work of Gaetz & Salpeter (1983) in which a very simple fit to the rate coefficient is proposed. Values of the fitting parameters are tabulated by these authors for a wide range of transitions and ions. We shall comment on some of these papers in later sections, but first we outline the aims and content of the present article.

Send offprint requests to: A. Burgess

1.1. Scope of the present work

We present a method which enables collision data for excitation of positive ions by electrons (i.e. cross sections and rate coefficients) to be critically assessed and compared at all energies and temperatures. The results are expressed in a compact form suitable for reduction of the large amount of collision data which is now accumulating in computerised data banks as well as in the literature and unpublished reports. The rate coefficient may be evaluated at all temperatures (which is of particular importance for rapidly evolving, non-equilibrium plasmas), and to within a likely error which, for all the cases we have examined, is much less than that of the original data. Results for whole isoelectronic sequences of ions may be combined into a single compacted form.

In the present paper we concentrate on data for ions of charge ≤ 30 (which covers almost all ions of astrophysical interest), so that, while magnetic interactions have to be taken into account, we do not need to consider the full relativistic effects of Lorentz transformation of electron velocities and this helps to simplify the formulae. Details of the modifications caused by the latter effects will be given elsewhere.

The method proposed here forms the basis of an interactive computer program with graphical display which was designed to be convenient to use not only by those working in atomic collision theory but also by plasma physicists and astrophysicists.

1.2. Checking tabulated data for errors

From the way collision data is normally tabulated (i.e. cross sections and collision strengths as functions of energy or, when thermally averaged, as functions of temperature) it is often difficult to detect mistakes such as printing errors. Data also needs to be checked for inconsistencies; such as, for example, when insufficient partial waves have been computed. This is particularly frequent at higher energies and gives data with incorrect high energy or temperature behaviour. This can also happen when physically invalid extrapolation procedures are used to allow for the contribution from high order partial waves. Our method allows such inadequacies in the data to be easily detected.

1.3. Scaling procedures

By using suitable scaling procedures it is possible to remove the main asymptotic energy (or temperature) dependence from the given data. The energy (temperature) is also scaled so as to become a dimensionless variable which ranges from 0 at threshold energy

© European Southern Observatory • Provided by the NASA Astrophysics Data System

1992A&A...254..436B

(zero temperature) to 1 at infinite energy (temperature). In this way the whole variation of a collision strength, for example, can be exhibited in a single graph since the energy is mapped onto the interval (0, 1), and the collision strength onto (0, y_{max}) with y_{max} finite. Such a graph can show where more, or less, data points are needed, so offering the possibility of economy in future calculations.

1.4. Fitting procedure

After scaling and plotting the data in the manner just described, the next step is to interpolate it. We find that a 5-point spline is satisfactory for collision strengths which do not have strong resonances (or which have been suitably averaged over the resonances), and for almost all rate coefficients. In this way a large number of data points, typically ~20, can be reduced to 5. In general the spline fit reproduces the original data to within a fraction of a percent. It is important to note that our fitting procedure allows data to be extrapolated correctly up to high energies or temperatures. This is not always true of the fitting formulae which have been proposed in the past.

The power of the present method arises from it being a smooth join of *local* fits in 4 separate energy regions: low, low-medium, medium-high and high.

1.5. Thermal averaging

In many plasmas the free electron distribution is very close to Maxwellian (Bohm & Aller 1947), and the excitation and de-excitation rate coefficients may be expressed in terms of the thermally averaged collision strength Y. Methods for carrying out the Maxwellian integration of Ω to give Y are discussed; careful account being taken of the high energy behaviour of Ω, which depends on the type of transition: optically allowed, optically forbidden, exchange or weakly allowed.

1.6. Non-Maxwellian averaging

If the free electron velocity distribution differs from Maxwellian only at high velocities (as for example in a low density plasma with a large temperature gradient) then, provided the departure from Maxwellian is expressed in the way suggested by Ljepojevic & Burgess (1990), the resulting excitation rate coefficients may be calculated with only slight modification of the above method.

1.7. Interactive programs

A first version of an interactive program implementing the methods described here for the analysis of rate coefficients was developed by one of us (A. B.), in collaboration with Jeff Payne, Jim Lang and Peter McWhirter at the Rutherford-Appleton Laboratory, for the Hewlett-Packard 45 system. A version for the Acorn BBC B, Master and Archimedes microcomputers has been further developed which handles both rate coefficients and collision strengths (Burgess 1992); this may also be run on the Apple MAC and IBM PC and compatibles.

2. The collision strength Ω

This dimensionless quantity was originally introduced by Hebb & Menzel (1940) in a classic paper devoted to electron impact excitation of O^{+2}. These authors remarked on the symmetry of Ω and noted that, for an electron colliding with a positive ion, it is finite at threshold energy. The name "collision strength" was suggested by Seaton (1953, 1955) and is now universally used.

In the following subsections we give the relationship between Ω and the cross-section Q, and then briefly discuss the overall dependence of Ω on the ion charge and projectile energy.

2.1. Definition of Ω

Ω is essentially the ratio of two areas (the cross-section and the square of the appropriate de Broglie wavelength of relative motion), viz.

$$\Omega_{ij} = \frac{4\pi\omega_i}{\lambda_i^2} Q(i \to j) . \tag{1}$$

The factor 4π is introduced for convenience, and the statistical weight ω_i of level i ensures that, from detailed balance, $\Omega_{ij} = \Omega_{ji}$.

Since the wave-number k is related to the wavelength λ by

$$k = \frac{2\pi}{\lambda} , \tag{2}$$

we have

$$Q(i \to j) = \frac{\pi\Omega_{ij}}{\omega_i k_i^2} . \tag{3}$$

This is the usual definition of Ω and is valid for incident particles with arbitrary mass. If Hartree's atomic units are used then k_i^2 is numerically equal to the reduced mass μ times the initial kinetic energy of relative motion in Rydbergs (13.6058 eV). For electron impact one can assume the target to be infinitely massive so that $\mu = m_e = 1$. Note that when Q is measured in πa_0^2 units ($8.79735\ 10^{-17}$ cm^2) the factor π no longer appears on the right hand side of (3).

2.2. Magnitude of Ω

For electron impact, Ω is typically of the order of unity, although this statement should not be taken too literally. In particular, we warn against assuming, as some astrophysicists have done, that when no data is available it is a reasonable approximation to calculate Q from (3) with $\Omega = 1$. The precise value of Ω depends of course on the transition, ion and impact energy. Resonances, which often occur at energies below the ionisation threshold, can cause Ω to vary widely from the background value. The present paper is not concerned with handling the large amount of data required to delineate complex resonance structures. For our purposes Ω always refers to the averaged collision strength in such cases.

It is interesting to note that the magnitude of Ω for proton impact is much larger (typically of the order of 10^6 at energies where Q is a maximum). This is because the cross-section depends mainly on the velocity of the incident particle and the magnitude of its charge, irrespective of its mass m, (since the transition is usually induced by the time-dependent electric field generated by the incident particle), so that the denominator in Eq. (1) is proportional to m^{-2} for comparable values of $Q(i \to j)$.

2.3. Charge dependence of Ω

As the ion charge number Z increases along an isoelectronic

© European Southern Observatory • Provided by the NASA Astrophysics Data System

1992A&A...254..436B

sequence the collision strength for a given transition eventually decreases. This behaviour of Ω simply reflects the "shrinkage" of the target as the nuclear attraction increases. Note that there may be exceptions near the neutral end of a sequence.

Non-relativistic perturbation theory shows that for large charge (and a given ratio of incident energy to transition energy),

$$\Omega \propto (Z + 1)^{-2} . \qquad (4)^*$$

[* Equation (4) only applies accurately to transitions involving valence electrons. For an inner-shell electron $(Z + 1)$ would be increased to some effective charge $Z_{\rm eff}$ seen by the electron.]

This is clear from the work on hydrogenic ions by Goldstein (1933) and Burgess et al. (1970) in which the Born and Coulomb-Born approximations were used respectively.

It is interesting to record that the Z-dependence shown in (4) was not immediately apparent to some early investigators. Aller & Menzel (1945), for example, tentatively surmised that Ω would *increase* like Z^2. They did, however, stress that only further calculations would throw light on the true Z-dependence of Ω, apparently being unaware of Goldstein's work.

It is sometimes useful also to note that, in general for $Z = 0$, the threshold value of Ω is zero.

2.4. *Energy dependence of Ω and types of transition*

For positively charged ions Ω is finite at threshold and with increasing energy it will in general be a complicated function of the electron energy E owing to the possibility of resonant capture of the colliding electron by excitation of the ion to a higher state. However, above the ionization threshold, and in particular as $E \to \infty$, Ω will tend to a simple limiting E-dependence which is determined by the dominant target-projectile interaction and hence by the type of transition. We now classify the transitions and give the high energy limiting behaviour, deduced from the Bethe, Born and Ochkur approximations:

1. Electric dipole, $\Omega \sim$ const. $\ln(E)$
2. Non electric dipole, non-exchange, $\Omega \sim$ const.
3. Exchange, $\Omega \sim$ const.$/E^2$.

Type 1 is associated with a non-zero oscillator strength f_{ij} (an optically allowed transition). For a few cases in which f_{ij} is very small, a slightly modified treatment may be required. These cases are classified as type 4 (see Sects. 3.4, 5.4 and 9.2).

Type 2 includes transitions which are induced by either an electric multipole interaction (i.e. E2, E3, . . .) or a magnetic multipole interaction (i.e. M1, M2, . . .). Such transitions are optically "forbidden". In certain rare cases the selection rules operate in such a way that an Ω of type 2 has a zero limiting value (as $E \to \infty$), due to vanishing of the first order Born matrix element. These cases are classified as type 5, and will be discussed elsewhere.

Type 3 involves a change in the spin of the ion (i.e. an intersystem transition) in which magnetic interactions are negligible. Such a transition can only occur through exchange between the incident and a bound electron. However, if magnetic effects are not negligible, so that intermediate coupling rather than LS coupling is required for the ion or the total system, then there will be no type 3 transitions. Thus spin-change transitions will often be of type 3 for ions with low Z, but as the charge increases they will become more predominantly of types 1, 2 or 4. Note that intersystem transitions of type 1 (or 4) are often referred to as "semiforbidden".

For theoretical data it is clear that the type of transition, and hence the high energy behaviour of Ω, depends on whether or not magnetic interactions are included in: (i) the Hamiltonian used to model the ion, (ii) the collision calculation. Thus for a given transition the high energy behaviour of collision strengths calculated in different approximations may not be the same (and the true behaviour, i.e. that of accurate experimental data, may be different again). In such cases, making allowance for how well the true physics of the ion is represented is a crucial part of the assessment of the data.

3. Scaling of Ω

It has been customary to plot or tabulate Q (or Ω) as a function of the colliding electron energy E. However, Tully (1978, 1980) showed that for intersystem transitions it is advantageous to remove the main E^{-3} dependence of Q by scaling; the scaled (or reduced) quantity having a relatively small overall variation between threshold and infinite energy. We extend this procedure to the other types of transition and make it more flexible by introducing an adjustable parameter C which is discussed in detail below. In this way considerable data storage economy can be achieved. Furthermore, by suitably scaling E, one can represent the entire variation of Q on a single graph or table.

The notation used is as follows:

Z_0	nuclear charge number
Z	ion charge number
$i \to j$	denotes excitation of the ion from state i to state j
E_i, E_j	colliding electron energy before, after excitation
I_i, I_j	ionization potential of the initial, final state
E_{ij}	transition energy (>0 for excitation)
f_{ij}	absorption oscillator strength (N.B. $\omega_i f_{ij} = -\omega_j f_{ji} = gf$)
$\Omega(E_j/E_{ij})$	collision strength as a function of E_j/E_{ij}
x	reduced energy ($= E_{\rm r}$)
y	reduced collision strength ($= \Omega_{\rm r}$)

All energies are expressed in terms of the Rydberg energy, $I_\infty = 13.6068$ eV, and all temperatures are in degrees Kelvin.

We now define the reduced variables x and y for the four types of transition. Note that x is defined to be zero at threshold ($E_j = 0$) and unity when $E_j = \infty$, also that $\Omega(0)$ = threshold value of Ω.

3.1. *Type 1*

$$x = 1 - \frac{\ln C}{\ln\left(\dfrac{E_j}{E_{ij}} + C\right)} \qquad (5)$$

$$y(x) = \frac{\Omega}{\ln\left(\dfrac{E_j}{E_{ij}} + \mathrm{e}\right)} \qquad (6)$$

$$\text{N.B.} \quad y(0) = \Omega(0) , \qquad (7)$$

$$\text{and} \quad y(1) = \frac{4\omega_i f_{ij}}{E_{ij}} \qquad (8)$$

(see Burgess & Tully 1978).

© European Southern Observatory • Provided by the NASA Astrophysics Data System

1992A&A...254..436B

3.2. Type 2

$$x = \frac{\left(\frac{E_j}{E_{ij}}\right)}{\left(\frac{E_j}{E_{ij}} + C\right)} \tag{9}$$

$$y(x) = \Omega . \tag{10}$$

N.B. $y(0) = \Omega(0)$, and $y(1)$ can in principle be obtained accurately by means of the Born approximation.

3.3. Type 3

$$x = \frac{\left(\frac{E_j}{E_{ij}}\right)}{\left(\frac{E_j}{E_{ij}} + C\right)} \tag{11}$$

$$y(x) = \left(\frac{E_j}{E_{ij}} + 1\right)^2 \Omega . \tag{12}$$

N.B. $y(0) = \Omega(0)$, and $y(1)$ can in principle be obtained by means of the Ochkur approximation.

3.4. Type 4

$$x = \text{as for type 1} \tag{13}$$

$$y(x) = \frac{\Omega}{\ln\left(\frac{E_j}{E_{ij}} + C\right)} . \tag{14}$$

N.B. $$y(0) = \frac{\Omega(0)}{\ln(C)} , \tag{15}$$

and $$y(1) = \text{as for type 1} . \tag{16}$$

4. Rate coefficient and thermally averaged collision strength

4.1. Definition of q

Let N_e be the total number of free electrons per unit volume. If the distribution of electron speeds $f(v)$ is Maxwellian, then

$$f(v) = \left(\frac{2}{\pi}\right)^{1/2} \left(\frac{m_e}{kT}\right)^{3/2} v^2 \exp\left(-\frac{m_e v^2}{2kT}\right) , \tag{17}$$

where

$$\int_0^\infty f(v)\,\mathrm{d}v = 1 . \tag{18}$$

The atomic $i \to j$ collision rate (i.e. transition probability per unit time) is given by $N_e q(i \to j)$ where

$$q(i \to j) = \int_0^\infty f(v_i) v_i Q(i \to j)\,\mathrm{d}v_i \tag{19}$$

is the rate coefficient. The collision rate per unit volume is $N_i N_e q$, where N_i is the number density of ions in level i. The atomic parameter $q(i \to j)$ is thus a measure of the frequency with which free electrons induce the transition $i \to j$ in a plasma at temperature T.

4.2. Definition of Y

We now transform from v_i to E_j, where E_j is the colliding electron kinetic energy after excitation has occurred, and rewrite (19) as follows:

$$q(i \to j) = 2\pi^{1/2} a_0 \hbar m_e^{-1} \left(\frac{I_\infty}{kT}\right)^{1/2} \exp\left(-\frac{E_{ij}}{kT}\right) \frac{Y_{ij}}{\omega_i} , \tag{20}$$

where

$$Y_{ij} = \int_0^\infty \Omega_{ij} \exp\left(-\frac{E_j}{kT}\right) \mathrm{d}\left(\frac{E_j}{kT}\right) \tag{21}$$

is the thermally averaged collision strength first introduced by Seaton (1953), and $2\pi^{1/2} a_0 \hbar m_e^{-1} = 2.1716\ 10^{-8}\ \mathrm{cm}^3\ \mathrm{s}^{-1}$.

The rate coefficient $q(j \to i)$ for the downward transition is given by

$$q(j \to i) = \left(\frac{\omega_i}{\omega_j}\right) \exp\left(\frac{E_{ij}}{kT}\right) q(i \to j) . \tag{22}$$

4.3. Temperature dependence of Y and types of transition

It follows from (21) that, when $T \to 0$, $Y \to \Omega(0)$, for all types of transition.

The high temperature limiting behaviour of Y follows from (21) and the energy dependence of Ω specified in Sect. 2.4. It depends on the type of transition as follows:

Type 1 (or 4)	$Y \sim$ const. $\ln(T)$
Type 2	$Y \sim$ const.
Type 3	$Y \sim$ const.$/T$

4.4. Charge dependence of Y

From Sect. 2.3 it is clear that, for a given transition and a given value of kT/E_{ij}, the quantity $(Z + 1)^2 Y$ will in general vary only slowly along an isoelectronic sequence, and will vanish when Z and T are both zero. This can be very useful when comparing, interpolating and compacting excitation data for whole sequences of ions; two examples are given in Sects. 7.5 and 8.2.

5. Scaling of Y

Taking into account the behaviour of Y as a function of T described in Sect. 4.4, reduced variables (analogous to those introduced in Sect. 3 for Ω as a function of E) may be used to map the whole variation of Y and T onto a finite range. Thus we now define x as the reduced temperature ($=T_r$), and y as the reduced Y ($=Y_r$), for the 4 types of transition; again incorporating an adjustable parameter C, which is not necessarily equal to that in Sect. 3. Note the x is defined to be zero when $T = 0$ and unity when $T = \infty$.

5.1. Type 1

$$x = 1 - \frac{\ln C}{\ln\left(\frac{kT}{E_{ij}} + C\right)} \tag{23}$$

$$y(x) = \frac{Y}{\ln\left(\frac{kT}{E_{ij}} + \mathrm{e}\right)} . \tag{24}$$

© European Southern Observatory • Provided by the NASA Astrophysics Data System

1992A&A...254..436B

N.B. $y(0) = \Omega(0)$, (25)

and $y(1) = \dfrac{4\omega_i f_{ij}}{E_{ij}}$. (26)

5.2. Type 2

$$x = \frac{\left(\dfrac{kT}{E_{ij}}\right)}{\left(\dfrac{kT}{E_{ij}} + C\right)} \tag{27}$$

$$y(x) = Y. \tag{28}$$

N.B. $y(0) = \Omega(0)$, (29)

and $y(1) =$ high energy limit of Ω. (30)

5.3. Type 3

$$x = \frac{\left(\dfrac{kT}{E_{ij}}\right)}{\left(\dfrac{kT}{E_{ij}} + C\right)} \tag{31}$$

$$y(x) = \left(\frac{kT}{E_{ij}} + 1\right) Y. \tag{32}$$

N.B. $y(0) = \Omega(0)$, (33)

and $y(1) = \int_0^\infty \Omega \, \mathrm{d}\left(\dfrac{E_j}{E_{ij}}\right)$. (34)

5.4. Type 4

$x =$ as for type 1 (35)

$$y(x) = \frac{Y}{\ln\left(\dfrac{kT}{E_{ij}} + C\right)}. \tag{36}$$

N.B. $y(0) = \dfrac{\Omega(0)}{\ln(C)}$, (37)

and $y(1) =$ as for type 1. (38)

6. Evaluation of Y

In the past, Ω has usually been fitted to functional forms chosen so that (21) can be evaluated analytically in terms of tabulated functions (exponential integrals etc.). When using a microcomputer, that approach is no longer of any real advantage since the evaluation of the analytic functions is often no quicker than numerical integration in (21). In contrast, our approach has been to aim first for the most efficient fitting of Ω (effectively precluding analytic evaluation of (21)), then to use numerical integration methods, carefully chosen so as not to lose any significant amount of the accuracy of the original data, and applicable for the whole range of T. We now discuss these numerical integration methods.

6.1. Trapezoidal rule

This is the method which has often been adopted in the past by those using the RMATRX package of Berrington et al. (1978). In the region of resonances Ω is evaluated at a large number of energies (typically several hundred) in order to delineate its complicated energy dependence. The aim is to use a sufficiently small steplength so that all resonances are accounted for. For convenience we now omit the subscript j from E_j so that E denotes the free electron energy after excitation. The contribution to Y from the interval $E_0 < E < E_1$ is then evaluated using the trapezoidal rule

$$\int_a^b \Omega \mathrm{e}^{-u} \, \mathrm{d}u = \left(\frac{\Delta}{2}\right)(\Omega_0 \mathrm{e}^{-a} + \Omega_1 \mathrm{e}^{-b}), \tag{39}$$

where $u = E/kT$, $a = E_0/kT$, $b = E_1/kT$ and $\Delta = b - a$. The first interval ($E_0 = 0$) contributes the amount

$$\int_0^\Delta \Omega \mathrm{e}^{-u} \, \mathrm{d}u = \left(\frac{\Delta}{2}\right)(\Omega_0 + \Omega_1 \mathrm{e}^{-\Delta}), \tag{40}$$

and this is the dominant contribution to Y when $T \to 0$. Since $(E_1 - E_0)$ is chosen independently of the temperature, it is seen that the trapezoidal approximation leads to a non-physical divergence in Y when $T \to 0$ ($\Delta \to \infty$). The method is therefore unsuitable at low temperatures.

6.2. Linear interpolation

Alternatively one can use linear interpolation to estimate Ω within an interval $E_0 < E < E_1$ and then evaluate the contribution to Y by analytic integration, i.e.

$$\Omega \approx \Omega_0 + (\Omega_1 - \Omega_0)\frac{(E - E_0)}{(E_1 - E_0)} \tag{41}$$

and

$$\int_a^b \Omega \mathrm{e}^{-u} \, \mathrm{d}u \approx [\Omega_0 - \Omega_1 \mathrm{e}^{-\Delta} - (\Omega_0 - \Omega_1)(1 - \mathrm{e}^{-\Delta})/\Delta]\mathrm{e}^{-a}. \tag{42}$$

In this case the integral over the first interval ($E_0 = 0$) contributes the following amount:

$$\int_0^\Delta \Omega \mathrm{e}^{-u} \, \mathrm{d}u \approx \Omega_0 - \Omega_1 \mathrm{e}^{-\Delta} - (\Omega_0 - \Omega_1)(1 - \mathrm{e}^{-\Delta})/\Delta. \tag{43}$$

This, unlike (40), tends to the correct limit as $T \to 0$ ($\Delta \to \infty$), namely Ω_0.

6.3. Gauss-Laguerre

The collision strength Ω is basically a function of E_j/E_{ij}, so that (21) is of the form

$$Y = \int_0^\infty e^{-u}\Omega(tu) \, \mathrm{d}u, \tag{44}$$

where $t = kT/E_{ij}$ and $u = E_j/kT$.

The Gauss-Laguerre method is ideally suited to this type of integral, provided Ω varies not too rapidly relative to the exponential term (so that Ω may be approximated by a polynomial in u). Thus it is the method we adopt for evaluating the non-resonance contributions to Y.

It can be applied in a straightforward manner, except perhaps when t becomes large. In this limit, the G-L points at which Ω is evaluated are all for $(E_j/E_{ij}) \to \infty$. This does not matter for type 2, since $\Omega \sim$ const. for large E_j/E_{ij}. Neither is it of much importance

© European Southern Observatory • Provided by the NASA Astrophysics Data System

1992A&A...254..436B

for types 1 and 4 since, for large E_j/E_{ij}, Ω increases like $\log(E_j/E_{ij}$ + const.), which, although not a polynomial, is slowly varying, so that the G-L method gives reasonable results for integrals of this type. For example, comparison with analytic evaluation shows that a 10-point G-L gives better than 1% accuracy when applied to

$$\int_0^\infty e^{-u} \log(tu + e)\,du,$$

no matter how large the value of t (the maximum error occurs for $t \sim 1000$). This is of course less accuracy than one would usually expect from the method (e.g. for $t < 2$, about 6-figure accuracy obtains), but it is adequate for the purpose, as we normally use 20 points with 5-, 10- and 15-point spot checks to assess the accuracy.

For type 3, however,

$$\Omega \propto \left(\frac{E_j}{E_{ij}} + 1\right)^{-2} \quad \text{for large } \frac{E_j}{E_{ij}}, \tag{45}$$

so that, in (44), when T is large, Ω varies more rapidly than the exponential term (and *not* approximately as a polynomial); in fact, the G-L value for

$$tY = \int_0^\infty \exp\left[-\left(\frac{E_j}{E_{ij}}\right)\Big/ t\right] \Omega\, d\left(\frac{E_j}{E_{ij}}\right) \tag{46}$$

tends to zero instead of $\int_0^\infty \Omega\, d\left(\frac{E_j}{E_{ij}}\right)$.

To allow for this, we write (for type 3 only)

$$tY = \int_0^\infty \exp\left[-\left(\frac{E_j}{E_{ij}}\right)\frac{t + C_1}{tC_1}\right]\left\{\Omega \exp\left(\frac{E_j}{C_1 E_{ij}}\right)\right\} d\left(\frac{E_j}{E_{ij}}\right), \tag{47}$$

where C_1 is a positive constant to be chosen. Applying the G-L procedure now gives results which tend uniformly (as $T \to \infty$) to a non-zero limiting value for tY. Ideally this should be $\int_0^\infty \Omega\, d\left(\frac{E_j}{E_{ij}}\right)$, i.e. $Y_r(T_r = 1)$, which we achieve as follows:

$$\text{Put} \quad v = \left(\frac{1}{t} + \frac{1}{C_1}\right)\frac{E_j}{E_{ij}}, \tag{48}$$

$$\text{then} \quad Y = (1 + t/C_2)^{-1} \int_0^\infty e^{-v}\left\{\Omega \exp\left[\frac{vt}{t + C_1}\right]\right\} dv, \tag{49}$$

where (for the moment) $C_2 = C_1$, and Ω is evaluated with

$$\frac{E_j}{E_{ij}} = \frac{vC_1 t}{t + C_1}. \tag{50}$$

This is now suitable for using G-L to calculate Y_r at any temperature, including $T = 0$ and $T \to \infty$. N.B. For $T = 0$, Eq. (49) correctly gives $Y_r = \Omega(0)$, which is independent of C_1, while for $T \to \infty$, Eq. (49) gives

$$Y = C_2 \int_0^\infty e^{-v}\{\Omega(vC_1)e^v\}\, dv. \tag{51}$$

We thus need to adjust C_1, C_2 by trial and error until

$$C_2 \int_0^\infty e^{-v}\{\Omega(vC_1)e^v\}\, dv = \int_0^\infty \Omega\, d\left(\frac{E_j}{E_{ij}}\right) \tag{52}$$

is satisfied as near as required, where G-L is used to evaluate the integral on the lhs, and any suitable method (usually a Newton-Cotes formula; Simpson, Boole, etc) used to evaluate the rhs. The latter is most conveniently done by first writing it in the form

$$\int_0^1 y[(C - 1)x + 1]^{-2}\, dx, \tag{53}$$

$$\text{where} \quad x = E_r = \left(\frac{E_j}{E_{ij}}\right)\Big/\left(\frac{E_j}{E_{ij}} + C\right) \tag{54}$$

$$\text{and} \quad y = \Omega_r = \left(\frac{E_j}{E_{ij}} + 1\right)^2 \Omega. \tag{55}$$

If $C_2 = C_1$ is maintained when making this adjustment, then a precise solution to (52) cannot usually be found, because the lhs reaches a maximum value slightly less than the rhs. We therefore relax the condition $C_2 = C_1$, use (52) to evaluate C_2 for any chosen C_1, then vary C_1 (with typical starting values for $C_1 = 0.67N^{1/2}$, where N is the number of G-L points used) until C_2/C_1 is as close to 1 as required. These optimal values of C_1, C_2 are then used in (49) for all required T. In effect, the method uses G-L for small T, and goes smoothly over to N-C at large T. Accuracy checks, carried out by varying the number of G-L points used and comparing with analytic results, again indicate that better than 1% accuracy is achieved no matter how large the value of t (the maximum error occurs for $t \sim 100$, and of course very much more accurate values obtain for $t \sim 1$).

6.4. *Non-Maxwellian excitation rates*

If the velocity distribution function may be expressed in the form suggested in the treatment developed by Ljepojevic & Burgess (1990), then, at a given point in the plasma where T is the temperature of the bulk of electrons,

$$Y = \int_0^\infty e^{-ug}\Omega(tu)\, du, \tag{56}$$

where $g(u)$ at that point is a given function (monotonic in u and asymptotic to unity for small u), which is obtained by solution of the Landau-Fokker-Planck equation.

Writing $v = ug$, we have

$$Y = \int_0^\infty e^{-v}\left(\frac{du}{dv}\right)\Omega(tu)\, dv, \tag{57}$$

so that the above integration methods may be used after obtaining $u(v)$ and $u'(v)$ by inverse interpolation of the given $v(u)$. A convenient method of doing this is to input g, as a tabulated function of v, into the procedure described in Sect. 7.2, to obtain g as a cubic spline in $V_r = v/(v + C)$ with C chosen to optimise the fit.

7. The microcomputer program OMEUPS

This is an interactive program with graphics for visually assessing and conveniently compacting collision strength data. It is easy to use even by non-specialists in atomic physics. The present version is in BBC BASIC and was written by one of us (A.B.) for ACORN microcomputers; viz. BBC models B, B+, M and Archimedes. With suitable emulators* it can also be run on the Apple MAC and IBM type micros.

© European Southern Observatory • Provided by the NASA Astrophysics Data System

1992A&A...254..436B

[* Available respectively from: Human-Computer Interface Limited, 25 City Road, Cambridge CB1 1DP; and M-Tec Computer Services, The Market Place, Reepham, Norfolk NR10 4JJ.]

OMEUPS has two branches labelled OMEGA and UPSILON. As the names suggest, OMEGA is for analysing energy-dependent collision strengths, while UPSILON deals with their thermally averaged counterparts. The compacting of data is done by a spline fitting technique which is outlined in the following section.

7.1. *Spline fitting of the scaled data*

We approximate $y(x)$, i.e. Ω_r or Y_r, over the domain $0 \leqslant x \leqslant 1$, by a cubic spline $y_s(x)$, with knots at $x = 0, 1/4, 1/2, 3/4$ and 1. The functional form of the resulting interpolating spline is given in the Appendix. The values of y_s at the knots are determined either by means of a least-squares fit to the data or by visual adjustment with computer graphics.

7.2. *OMEGA branch*

After inputting the data (i.e. E_j and Ω_{ij}) and an initial estimate for C, the collision strength is transformed to Ω_r and displayed as a function of E_r. By modifying the value of C one can change the distribution of data points on the plot so as to obtain a reasonably even distribution in x (increasing C pushes the points to lower x, and vice versa).

The least-squares spline curve is then drawn on the screen and can be compared with the original data points. The possibility exists of adjusting the spline curve manually, by moving a cursor on the screen, to change one or more of the five knot-values $y_s(x_i)$ ($i = 1, \ldots 5$). This may be necessary if there are insufficient data points, or if some of the data points are assessed as of low accuracy (as an alternative such points may be given reduced weight in the least-squares calculation).

The rms error of the fit, together with the nodal values $y_s(x_i)$ ($i = 1, \ldots 5$) appear on the screen. Finally, by altering C and repeating the least-square fit, it is possible to minimise the rms error. This is typically found to be less than 1%.

The fitted Ω may then be averaged over the distribution function, to produce the corresponding Y, using the methods described in Sect. 6.

7.3. *UPSILON branch*

If Ω shows complicated resonance structure then it cannot be treated by OMEUPS in its present form. However the thermally averaged collision strength Y will in general be a smoothly varying function of T, and for this the present fitting procedure is ideally suited. The scaled quantity Y_r is plotted against the reduced temperature T_r and then approximated by an interpolating 5-point cubic spline in exactly the same way as Ω_r. By varying the parameter C and minimising the rms error one can optimise the fit.

7.4. *Treatment of pseudo resonances*

Close coupling codes such as RMATRX often produce spurious "pseudo" resonances in Ω if pseudo orbitals are included in the calculation. These fluctuations usually occur at energies above the region of true resonances, and our method provides a simple means of removing their effect.

We illustrate this by considering the type 2 transition $3s^2\,{}^1S - 3s3d\,{}^1D$ in Si^{+2}, for which Dufton has performed a 12-state close coupling calculation (Dufton, private communication 1982; see also Dufton et al. 1983; Dufton & Kingston 1989). Dufton's results have now replaced those of Baluja et al. (1980, 1981b) in the atomic data bank at The Queen's University of Belfast.

Energy-averaged collision strengths for some of the transitions, in the range $0 \leqslant E_j \leqslant 1$, are given in Dufton & Kingston (1989). This is a useful way of compacting collision data which, because of resonance structure, is very voluminous. The averaging was carried out in 10 contiguous energy intervals ranging from (0, 0.05) to (0.7, 1.0). We have corrected a misprint in their Table 4, where the last interval is given as (0.7, 10.0). Only the first two energy bins lie within the region of true resonances ($E_j < 0.0974$), and above this their collision strength varies smoothly. In Fig. 1 we plot Ω_r at the midpoint of each bin; we also include 19 additional data points corresponding to values of Ω from the QUB data bank at energies in the range $0.8894 \leqslant E_j \leqslant 8.4894$, and the high energy limit value $\Omega_r(1) = 1.646$. This was obtained using the Born approximation, and details of our calculation will be given elsewhere.

By making a spline fit we are able to remove the effect of the large pseudo resonance at $E_r \sim 0.6$. This is shown in Fig. 2, where the original collision strength is plotted as a function of E_j together with a curve generated by the spline fit. The present technique is seen to be a convenient way of correcting the unphysical fluctuation in Ω.

It also averages over the jump in Ω at low energies ($E_r \sim 0.1$) which is caused by real resonances. In order to check whether this introduces any substantial error, we used the Ω_r spline to calculate Y, and compared with the values of Y given by Dufton & Kingston (1989) for the range $3.8 \leqslant \log T \leqslant 5.2$. Agreement to within 3% was found.

It is interesting to compare the data bank results shown in Figs. 1 and 2 with the high energy limiting value. The close coupling calculation included only partial waves with $L \leqslant 12$, and this is insufficient to ensure convergence at the highest energies considered. The data bank has a program for approximating the high order partial wave contributions which uses the same method for

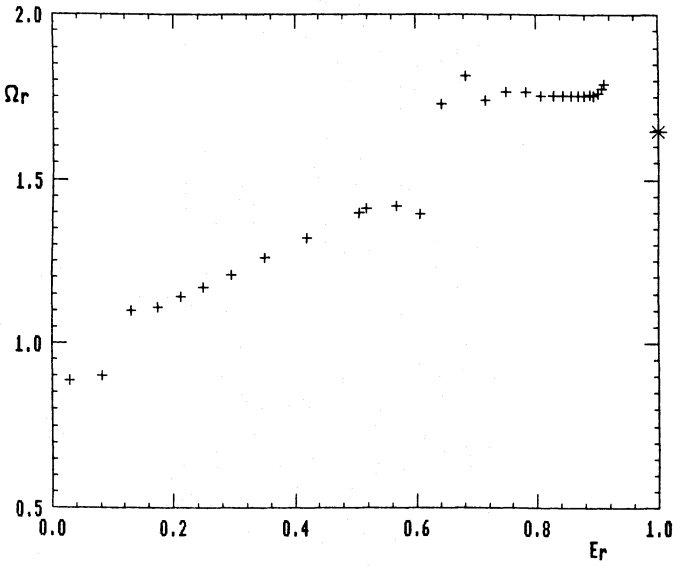

Fig. 1. $Si^{+2}(3s^2\,{}^1S - 3s3d\,{}^1D)$. RMATRX data showing pseudo resonance near $E_r = 0.6$. * Born limit. $C = 0.55$

© European Southern Observatory • Provided by the NASA Astrophysics Data System

1992A&A...254..436B

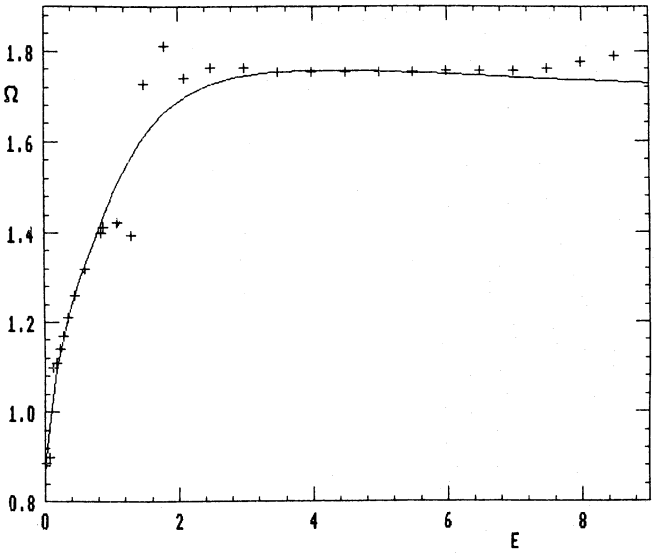

Fig. 2. OMEUPS averaging out of pseudo resonances, from data points shown in Fig. 1

allowed and forbidden transitions i.e. it assumes that $\Omega_{L+1}/\Omega_L \sim$ constant as $L \to \infty$. While there is no theoretical justification why this should apply to type 2 transitions, one can see from Fig. 1 that in the present case it does appear to work remarkably well, although there is some indication that it slightly overestimates at the highest energies.

Finally, on spline fitting Y_r with $C = 1$ and knot values 0.884, 1.236, 1.449, 1.629 and 1.652, we find that Y for this transition can be obtained with no significant error above that of the original data.

7.5. *Treatment of isoelectronic sequences of ions*

Suppose that the above procedures have been used to obtain the spline knot values of $Y_r(T_r)$, ($T_r = 0, 1/4, 1/2, 3/4, 1$), for a particular transition in isoelectronic ions of varying charge Z. From Sect. 4.4, we see that the values of $(Z+1)^2 Y_r$, for each given T_r, should vary smoothly with Z and stay finite for all Z, so that they may again be interpolated and fitted, this time to a reduced Z variable of the form

$$Z_r = \frac{Z}{Z + C}. \tag{58}$$

Note that, if we include the neutral atom case (but not negative ions), the range of the reduced independent variable is again (0, 1), and that the adjustable constant C may be different from that used in the first fitting (to T_r, see Sect. 5).

Thus, defining

$$Y_{rr}(T_r, Z_r) = (Z+1)^2 Y_r(T_r), \tag{59}$$

we see that the overall procedure is a two dimensional spline fit to the surface Y_{rr} over the unit square $0 \leq T_r \leq 1$, $0 \leq Z_r \leq 1$. This gives a 5×5 set of spline knot values for Y_{rr} from which, in principle, the rate coefficient may be obtained for all temperatures and all charges.

As an example, in this section we consider Li-like ions, for which there is a good set of data (see e.g. Cochrane & McWhirter 1983), limiting ourselves to ion charges such that full relativistic effects may be neglected (see Sect. 1.1.). In Sect. 8.2, a further worked example is given for Be-like ions, and applied in detail to N^{+3}.

7.5.1. 2s-2p transitions in Li-like ions

We consider data for the isoelectronic ions Be^+, C^{+3}, O^{+5}, Mg^{+9}, Ar^{+15} and Fe^{+23}, taken from: Hayes et al. (1977); Merts et al. (1980); Cochrane & McWhirter (1983); Gallagher & Pradhan (1985); Burgess et al. (1988, 1989); Zhang et al. (1990). On using OMEUPS, the data appeared to contain no inconsistencies or discrepancies.

For this range of ion charge we need only fit

$$\Omega(2s, 2p) = \Omega(2s_{1/2}, 2p_{1/2}) + \Omega(2s_{1/2}, 2p_{3/2}) \tag{60}$$

since, to a good approximation,

$$\Omega(2s_{1/2}, 2p_{3/2}) = 2\Omega(2s_{1/2}, 2p_{1/2}). \tag{61}$$

To obtain the spline fit to Ω_r (as described in Sect. 7.2), a common value of $C = 4$ was taken which, although not quite optimal for each ion, gave very good fits to the data; the rms errors being 0.87%, 0.58%, 0.90%, 0.18%, 0.32% and 0.29% respectively.

These fits to Ω_r were used to calculate the Y, which were in turn used (see Sect. 7.3) to obtain the spline fit to Y_r for each of the ions. Again, a common value of $C = 4$ was found to give very accurate fits to the Y; the rms errors being 0.20%, 0.45%, 0.40%, 0.59%, 0.72% and 0.77% respectively.

The spline knot values of $Y_{rr} = (Z+1)^2 Y_r$ thus obtained were then fitted (as a function of $Z_r = Z/(Z+4)$, separately for each value of T_r (=0, 1/4, 1/2, 3/4, 1). Again a common value of $C = 4$ gave a very good fit; the rms errors being 0.42%, 0.18%, 0.25%, 0.23% and 0.97% respectively.

Figure 3 shows the original data for $Y_{rr}(T_r, Z_r)$, the first spline curve fit to it for each of the 6 ions, and the final double spline surface fit to all of the data.

The final result is that excitation rate coefficients for *all* 23 ions (Be^+ to Fe^{+23}) may be obtained at *all* temperatures, with negligible error additional to that of the original data, from the following expression:

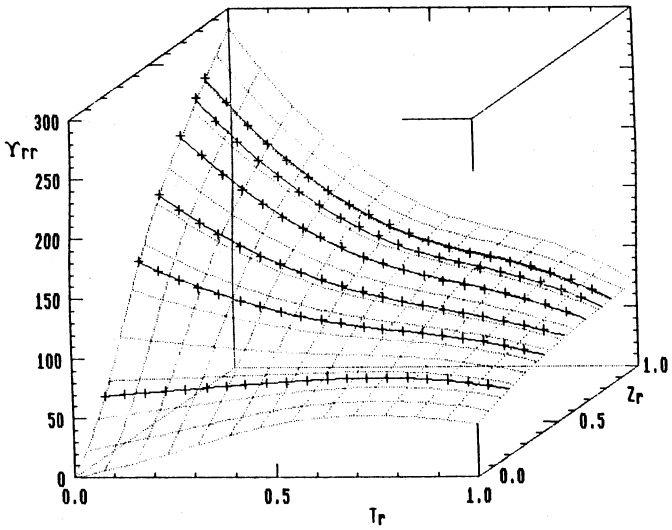

Fig. 3. Li-like ions ($2s - 2p$). Plot of Y_{rr} against reduced temperature T_r and reduced ion charge Z_r

© European Southern Observatory • Provided by the NASA Astrophysics Data System

1992A&A...254..436B

$$Y(2s, 2p) = (Z + 1)^{-2} \ln\left(\frac{kT}{E} + e\right) \cdot \mathrm{spline}(P_1, P_2, P_3, P_4, P_5, T_r), \quad (62)$$

where

$$P_n = \mathrm{spline}(S_{1n}, S_{2n}, S_{3n}, S_{4n}, S_{5n}, Z_r) \quad (1 \leqslant n \leqslant 5), \quad (63)$$

$$T_r = 1 - \frac{\ln(4)}{\ln\left(\frac{kT}{E} + 4\right)}, \quad (64)$$

$$Z_r = \frac{Z}{Z + 4}, \quad (65)$$

the function spline (a, b, c, d, e, x) is given in the Appendix, E is the 2s − 2p excitation energy of the ion, and the S_{mn} are as in Table 1.

With modifications to include full relativistic effects and departure from approximation (61), the above fit is extendable to cover the whole range $1 \leqslant Z \leqslant 89$. This will be detailed elsewhere.

8. Comparison with other fits

Previous fitting techniques have often been based on simple global analytic expressions, with adjustable parameters determined by the method of least squares. Such fits are useful for interpolating collision strengths that vary slowly with energy or temperature. However, unlike the present approach, they may not be suitable for extrapolating beyond the range in which the original data was calculated. This drawback is apparent in the examples which follow.

8.1. An $\Omega(E)$ fit

A functional form that is widely used for fitting collision strengths which have no resonance structure is the following:

$$\Omega = \sum_{N=0}^{N_{\max}} C_N X^{-N} + D \ln X \quad (66)$$

where $X = E_i/E_{ij}$.

The integration in (21) can be performed analytically to give

$$Y = C_0 + \left\{\sum_{N=1}^{N_{\max}} y C_N E_N(y) + D E_1(y)\right\} e^y, \quad (67)$$

where $y = E_{ij}/kT$ and $E_N(y)$ is the exponential integral of order N (see Abramowitz & Stegun 1964).

As an example we consider the 2-state close coupling calculation by Ho & Henry (1983) for the $2p^3\,{}^4S - 2p^2 3s\,{}^4P$ type 1 transition in O^+. These authors give the collision strength graphically over the range $0.86 \leqslant E_i \leqslant 6$. They were able to fit their results to within 5% by the expression (66), with $N_{\max} = 2$, $C_0 = -2.173$, $C_1 = 4.090$, $C_2 = -1.510$ and $D = 1.465$. We have used this to evaluate Ω at 10 energies and the results for Ω_r are shown in Fig. 4. Also shown is our spline fit to these values of Ω_r, which, it should be noted, do not tend towards the true high energy limit. $C = 1.7$ gave a minimum rms error of 0.20%. We then used OMEUPS to calculate Y at 10 temperatures and made an optimised spline fit to the reduced data points by choosing $C = 3.8$ (rms = 0.25%, see Fig. 5). Table 2 compares values of Y from (67) and from OMEUPS; they are seen to differ by not more than 3%.

Ho & Henry (1983) state that (67) should not be used for $T > 10^6$. The reason for this is that while (66) has the correct high energy dependence (namely $\propto \ln X$), the value 1.465 for the coefficient D differs from the Bethe limit value $4gf/E_{ij} = 0.800$. In Fig. 6 we retain only the data points from Fig. 4 which correspond to energies $E_i \leqslant 6$ and, when making the spline fit, include the correct high energy limit point. This corresponds to $f = 0.086$, which is the dipole length oscillator strength given by Ho & Henry. The spline curve in Fig. 6 bridges the gap between the low energy data points and the Bethe limit and we surmise that the resulting fit to Y_r shown in Fig. 7 (with $C = 3.8$ and knot values 0.4070, 0.4089, 0.4619, 0.5806, 0.8014) should allow one to make reliable estimates of Y at all temperatures.

8.2. Fits for $Y(T)$

Numerical integration is used to calculate Y when Ω contains resonance structure or if it has not been approximated by an analytic expression. Y is a slowly varying function of temperature and

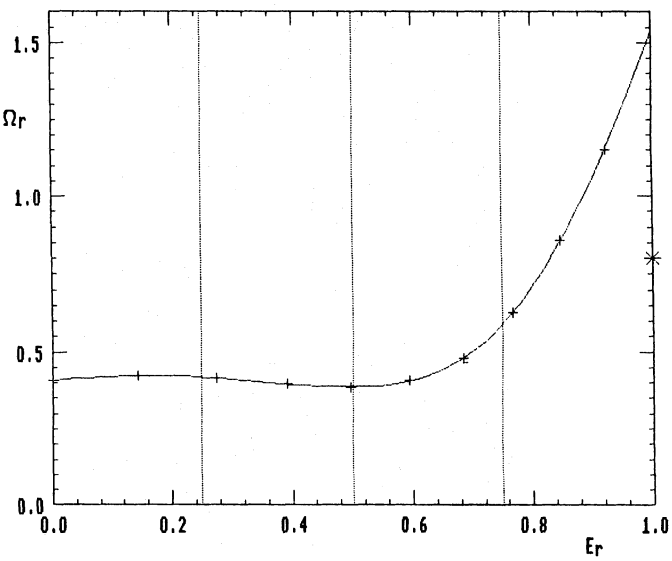

Fig. 4. $O^+(2p^3\,{}^4S - 2p^2 3s\,{}^4P)$. Optimised fit to Ω_r data points generated by the simple functional form of Ho & Henry (1983). N. B. The data do not tend to the Bethe limit *

Table 1. Spline knot values S_{mn} for use in (63) to give $Y(2s, 2p)$ in all Li-like ions of charges 1 to 23

m/n	1	2	3	4	5
1	0.000	21.88	45.01	51.99	44.40
2	67.89	68.12	68.88	68.23	57.26
3	167.8	124.4	97.79	83.27	64.47
4	234.6	162.1	118.5	97.00	68.81
5	284.2	186.8	130.2	107.0	70.76

Table 2. Y for $O^+(2p^3\,{}^4S - 2p^2 3s\,{}^4P)$. Calculated; (a) analytically from (67), (b) using OMEUPS

$\log(T)$	3.0	3.5	4.0	4.5	5.0	5.5	6.0
Y(a)	0.408	0.411	0.419	0.434	0.462	0.551	0.874
Y(b)	0.408	0.409	0.412	0.421	0.451	0.553	0.873

© European Southern Observatory • Provided by the NASA Astrophysics Data System

1992A&A...254..436B

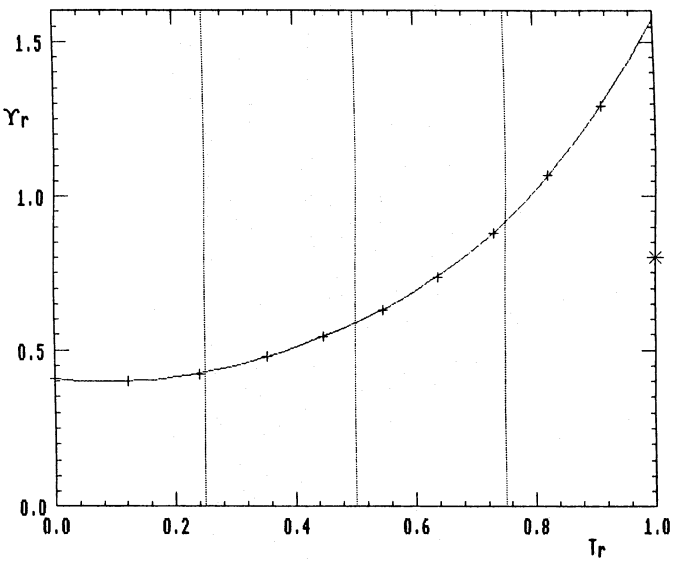

Fig. 5. $O^+(2p^3\,{}^4S - 2p^2 3s\,{}^4P)$. Optimised fit to Y_r data generated by OMEUPS from the curve in Fig. 4

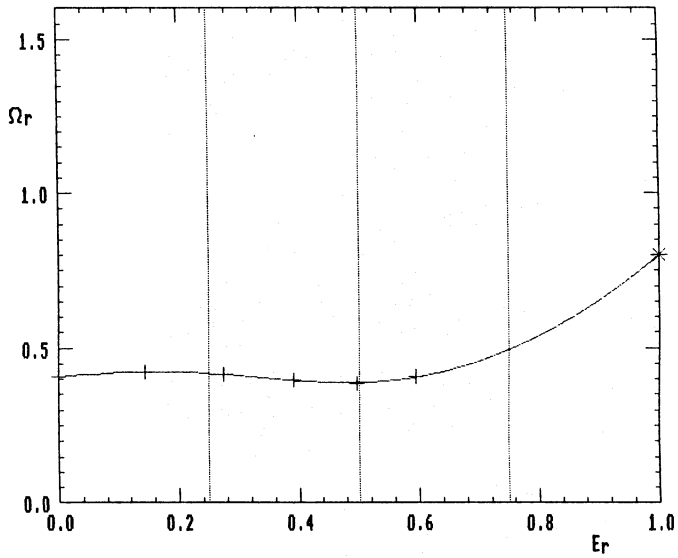

Fig. 6. As in Fig. 4, but omitting data points at energies $E_i > 6$ and including the limit point $\Omega_r(1) = 0.800$. To match Fig. 4, $C = 1.7$ was used, which gives a not quite optimal rms of 0.17%

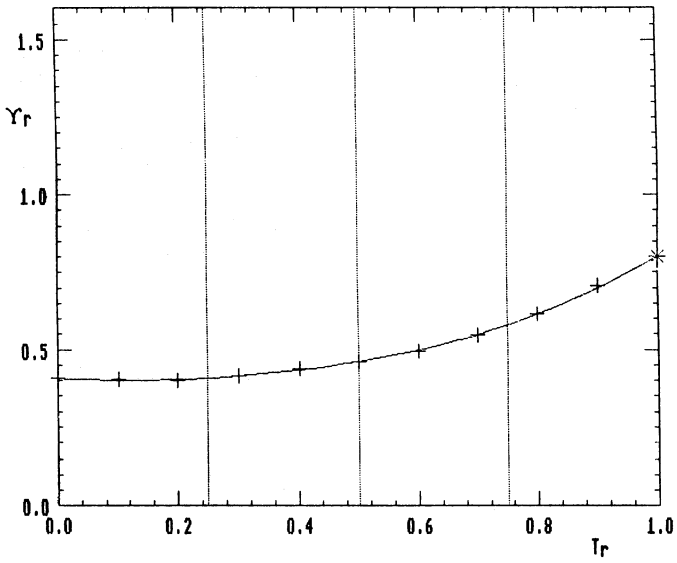

Fig. 7. As in Fig. 5, but with data points generated from the curve in Fig. 6. To match Fig. 5, $C = 3.8$ was used, which gives a not quite optimal rms of 0.4%

therefore amenable to analytic approximation. It is customary to use a fit that is valid only in a restricted temperature range centred on the temperature at which the ion has maximum abundance under conditions of ionisation equilibrium.

We consider the $2^1S - 2^1P$ transition in N^{+3} which raises a number of interesting points related to the interpolation of data, not only in temperature, but also in atomic number. Since this ion has not been the object of detailed quantal calculations we estimate Y for it by interpolating the data available for other ions in the Be-like isoelectronic sequence, namely C^{+2}, O^{+4}, Ne^{+6} and Si^{+10}.

Berrington et al. (1981) used the close coupling and Coulomb Born approximations for 29 transitions in these ions. Later they extended their calculations of Ω to higher energies and gave reliable fits for the optically allowed transitions, including the one we are interested in (Berrington et al. 1985a). They also performed thermal averaging and tabulated the resulting Y at temperatures in the range $\log(T_m) \pm 0.8$, where $\log(T_m) = 4.9$, 5.3, 5.8 and 6.2 for C^{+2}, O^{+4}, Ne^{+6} and Si^{+10} respectively. These values for T_m are taken from Jordan (1969).

Keenan et al. (1986) used a quadratic in Z_0 to fit the data for C^{+2}, O^{+4}, Ne^{+6} and Si^{+10}. More precisely, their procedure was to fit, to a quadratic in Z_0, the values of Y for temperatures

$$T = cI_P Z_0\,, \tag{68}$$

where I_P is the ionisation potential (in eV) and c is a constant chosen so that $\log(T)$ lies in the range used by Berrington et al. (1985a). In this way Keenan et al. were able to interpolate along the isoelectronic sequence and obtain Y for each of the 29 transitions considered by Berrington et al. (1985a). Finally, they used the following cubic polynomial to fit their data for transitions in N^{+3} and other ions in the sequence:

$$Y(T) = a_0 + a_1 t + a_2 t^2 + a_3 t^3\,, \tag{69}$$

where $t = \log(T)$. The values of the coefficients a_i for $N^{+3}(2^1S, 2^1P)$ are: $a_0 = 20.09$, $a_1 = -7.490$, $a_2 = 0.83727$ and $a_3 = 0$.

Gaetz & Salpeter (1983) adopted quite a different fitting formula, namely

$$Y(T) = \alpha\left(\frac{T}{T_m}\right)^{\beta}. \tag{70}$$

They thermally averaged the collision strengths given by Berrington et al. (1981), and then used (70) to fit their results. By graphical interpolation of α and β for $Z = 2$, 4, 6 and 10, we find $\alpha = 3.85$ and $\beta = 0.092$ for $N^{+3}(2^1S, 2^1P)$. These values differ from those given by Gaetz & Salpeter ($\alpha = 4.03$ and $\beta = 0.157$) suggesting that they used a different way of interpolating along the isoelectronic sequence. We note that their tabulated β is not a smoothly varying function of Z as it presumably ought to be.

© European Southern Observatory • Provided by the NASA Astrophysics Data System

1992A&A...254..436B

In order to compare our fitting procedure with the aforementioned methods, we proceeded as follows. The $Y(2^1S, 2^1P)$ data from Berrington et al. (1985a) for $Z = 2, 4, 6$ and 10 were fitted by UPSILON to give the spline knot values of $Y_r(T_r)$ shown in Table 3. It was clearly simpler to use the same value of C for the different ions, but in all cases this was very close to the optimal value. The maximum rms error was 0.29%.

As in Sect. 7.5, we then fitted the scaled quantities $(Z+1)^2 Y_r(T_r)$ to 5-point splines in $Z_r = Z/(Z+C)$, for each value of T_r, so the $Y(2^1S, 2^1P)$ can now be obtained for any Be-like ion with charge in the range $2 \leqslant Z \leqslant 10$, from

$$Y = (Z+1)^{-2} \ln\left(\frac{kT}{E} + e\right) \text{spline}(P_1, P_2, P_3, P_4, P_5, T_r), \quad (71)$$

where

$$P_n = \text{spline}(S_{1n}, S_{2n}, S_{3n}, S_{4n}, S_{5n}, Z_r) \quad (1 \leqslant n \leqslant 5), \quad (72)$$

$$T_r = 1 - \frac{\ln(2.2)}{\ln\left(\frac{kT}{E} + 2.2\right)}, \quad (73)$$

$$Z_r = \frac{Z}{Z+4}, \quad (7.4)$$

E is the $2^1S - 2^1P$ excitation energy of the ion, the function spline(a, b, c, d, e, x) is given in the Appendix and the S_{mn} are as in Table 4.

In particular, for N^{+3}, by using (72) with $Z = 3$, we obtain for the P_n (i.e. the spline knot values of $16 Y_r(T_r)$), the values 51.65, 49.54, 45.30, 40.54 and 33.04 corresponding to $T_r = 0$, 1/4, 1/2, 3/4 and 1 respectively. These can then be used in (71) to determine Y for N^{+3} for arbitrary T. In Fig. 8 we plot Y, calculated in this way, as a function of $\log(T)$. Also shown are the values of Y given by the fitting formulae (69) and (70). While there is reasonable agreement (better than 10%) for temperatures in the range $4.4 \leqslant \log T \leqslant 6.0$, only the present method provides a reliable means of estimating $Y(T)$ for arbitrarily small or large values of T.

Table 3. Be-like ions: Spline fit to $Y(2^1S, 2^1P)$ with $C = 2.2$. (Z is the ion charge)

Z	$Y_r(0)$	$Y_r(1/4)$	$Y_r(1/2)$	$Y_r(3/4)$	$Y_r(1)$
2	3.869	3.952	3.890	3.804	3.303
4	2.657	2.452	2.152	1.815	1.417
6	1.839	1.625	1.366	1.070	0.7909
10	0.9926	0.8570	0.6905	0.5006	0.3502

Table 4. Spline knot values S_{mn} for use in (72) to give $Y(2^1S, 2^1P)$ in all Be-like ions of charge 2 to 10

m/n	1	2	3	4	5
1	0.000	3.506	7.012	10.52	14.02
2	22.67	25.05	26.90	28.66	26.51
3	66.43	61.30	53.80	45.37	35.43
4	129.8	112.0	89.06	63.06	43.42
5	199.7	181.8	131.5	78.85	49.13

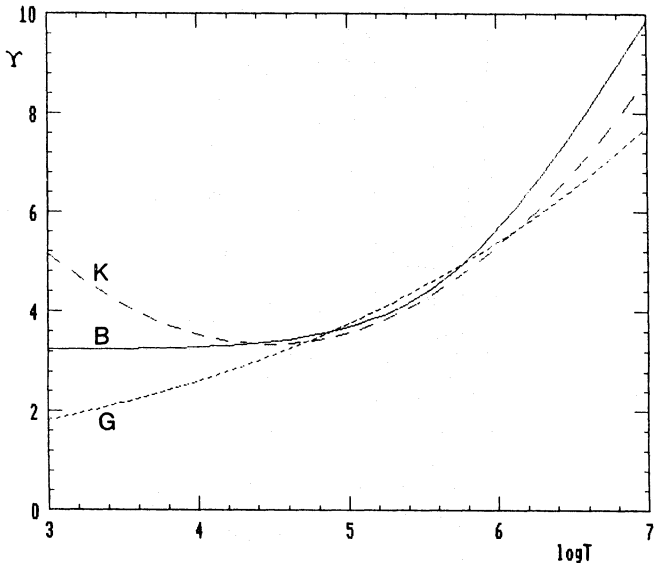

Fig. 8. $N^{+3}(2s^2\,{}^1S - 2s2p\,{}^1P)$. Comparison of fitting techniques. *K*, Keenan et al. (1986); *G*, Gaetz & Salpeter (1983); *B* present method. Only *B* is correct over the whole range of log *T*

9. Further examples of the method

So far we have concentrated attention on type 1 and type 2 transitions. For completeness we now analyse cases of type 3 and type 4 transitions. Together with the previous examples these highlight certain features of the OMEUPS program. They show, for example, that a knowledge of the high-energy limit point greatly enhances confidence in the fit. However, it appears from the numerous cases we have tested so far that, even when the limiting value is unknown, the present method provides physically meaningful results at all energies and temperatures.

9.1. A type 3 transition

We consider the transition $1s^2\,{}^1S - 1s2p\,{}^3P$ in O^{+6}. Figure 9 is a plot of $\Omega_r(E_r)$ based on the tabulated data from Sampson et al. (1983), who used the Coulomb Born Oppenheimer (CBO) approximation (see Burgess et al. 1970), so consequently their collision strength Ω is a smoothly varying function of energy.

When making the spline fit shown in Fig. 9 ($C = 3.6$, rms = 0.18%), we took account of the Ochkur high energy limit $E_j^2\Omega = 43.0$. (Tully 1980). We then used the program to calculate $Y(T)$ at 10 temperatures, as described in Sect. 6.3, with 20 G-L integration points. The resulting graph of $Y_r(T_r)$ is shown in Fig. 10. The program automatically evaluates the integral $\int_0^\infty \Omega \, dE_j$ and obtained the value 1.204. This determines the high temperature limit point (see Eq. (34)), which is denoted by an asterix in Fig. 10. The value of C was varied in order to optimise the spline fit ($C = 2.4$, rms = 0.39%).

Finally, we show how OMEUPS can be used to compare these values of Y with those given by Tayal & Kingston (1984). The latter used the RMATRX package of Berrington et al. (1978) to calculate $\Omega(E)$, then by numerical integration obtained Y at temperatures in the range $6\ 10^4 \leqslant T \leqslant 6\ 10^6$. Figure 11 shows the RMATRX values of Y_r together with CBO points generated from the spline fit in Fig. 10. Note that a value of C (=0.2) much smaller than in

© European Southern Observatory • Provided by the NASA Astrophysics Data System

1992A&A...254..436B

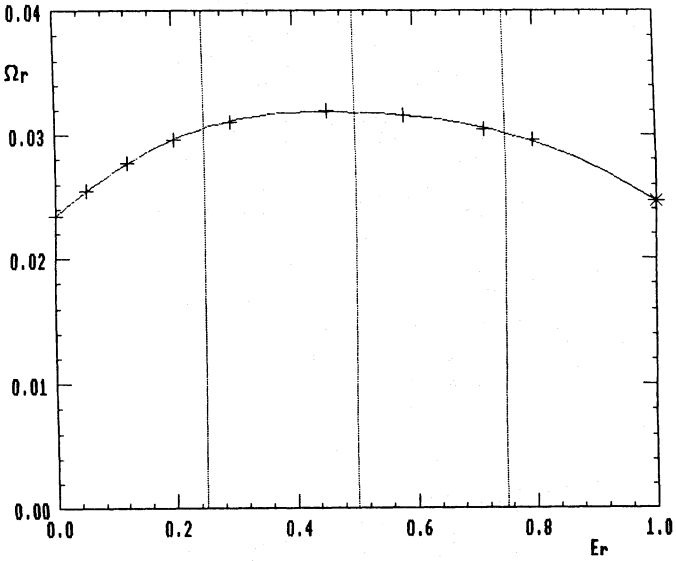

Fig. 9. $O^{+6}(1s^2\,{}^1S - 1s2p\,{}^3P)$. CBO data from Sampson et al. (1983); Ochkur high energy limit from Tully (1980). $C = 3.6$ with knot values 0.02342, 0.03059, 0.03186, 0.03021, 0.02463

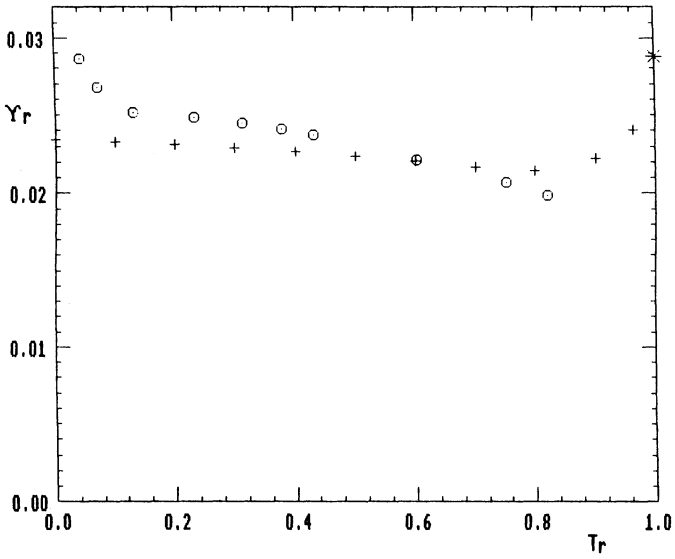

Fig. 11. $O^{+6}(1s^2\,{}^1S - 1s2p\,{}^3P)$. Comparison of Y_r data from: + the fit in Fig. 10; ⊙ Tayal & Kingston (1984). $C = 0.2$

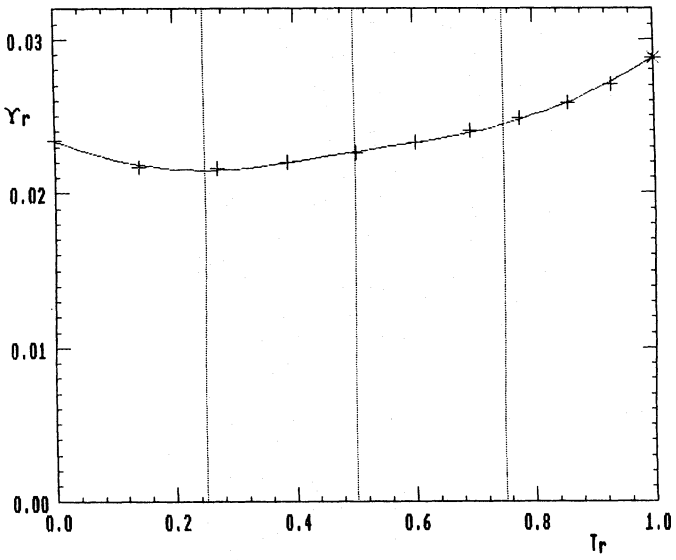

Fig. 10. $O^{+6}(1s^2\,{}^1S - 1s2p\,{}^3P)$. Data for $T_r < 1$ from OMEUPS using the Ω_r spline fit of Fig. 9. $C = 2.4$ with knot values 0.02338, 0.02148, 0.02265, 0.02443, 0.02875

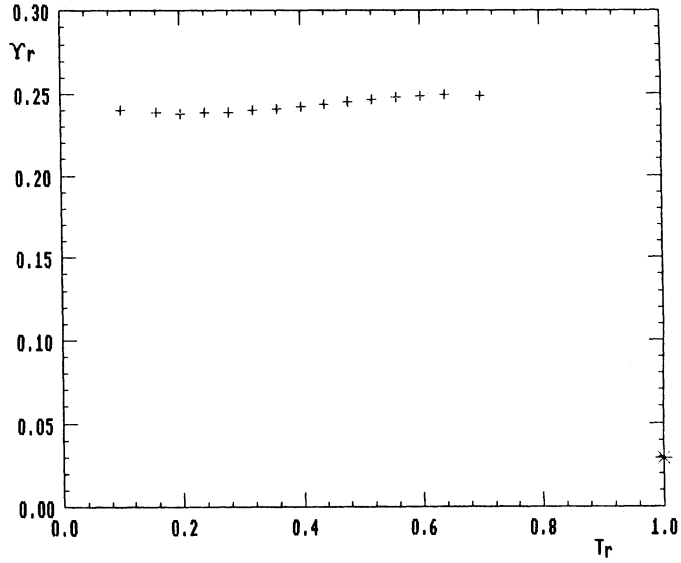

Fig. 12. $Si^{+2}(3s^2\,{}^1S - 3s4p\,{}^1P)$. Transition with a small oscillator strength, treated as type 1. Data from parametric fit given in Dufton and Kingston (1989). * Bethe limit. $C = 1.2$

Fig. 10 was chosen in order to display the data points spread across the whole of the figure.

There is reasonable (~25%) overall agreement between the CBO and RMATRX results. At low temperatures the close coupling data points lie above those of the weak coupling approximation. This shows how the contribution from resonances raises the collision strength above its background value. As a consequence (since it is the overall integral of Ω), one would expect the RMATRX limit $Y_r(1)$ to be greater than the CBO value. However, the reverse seems to be the case, and this raises some doubt about the high temperature fall off of the RMATRX values.

9.2. *A type 4 transition*

We use the parametric fit from Dufton & Kingston (1989) to obtain $Y(T)$ for the $3s^2\,{}^1S - 3s4p\,{}^1P$ transition in Si^{+2}. This is an optically allowed transition with the small gf value of 0.0117 (Baluja & Hibbert 1980) and so is a candidate for type 4.

For comparison, we first treat it as type 1 and plot it as such in Fig. 12. Here something appears to be amiss since the data points do not tend towards the Bethe limit at $T_r = 1$. Unfortunately we cannot explore the region $0.75 < T_r < 1$ with Dufton & Kingston's fit since it has a limited range of validity.

We therefore make a type 4 plot in Fig. 13 and here the data points line up satisfactorily with the high temperature limit which is,

© European Southern Observatory • Provided by the NASA Astrophysics Data System

1992A&A...254..436B

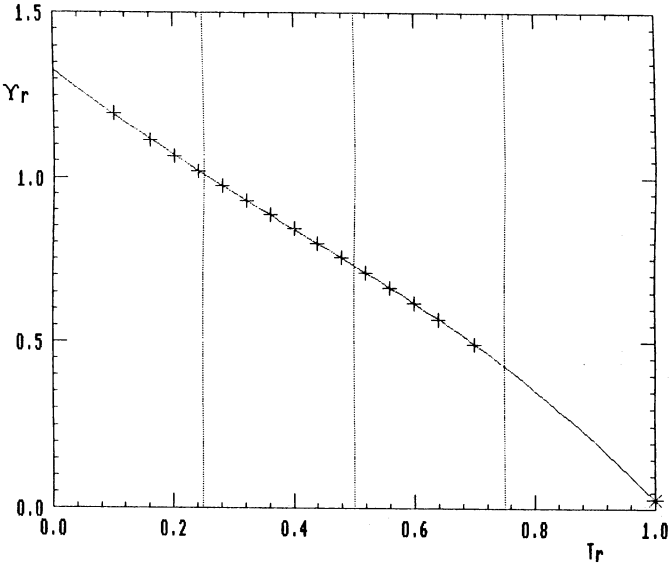

Fig. 13. As in Fig. 12, but treated as type 4. $C = 1.2$ with knot values 1.327, 1.008, 0.7305, 0.4269, 0.02939

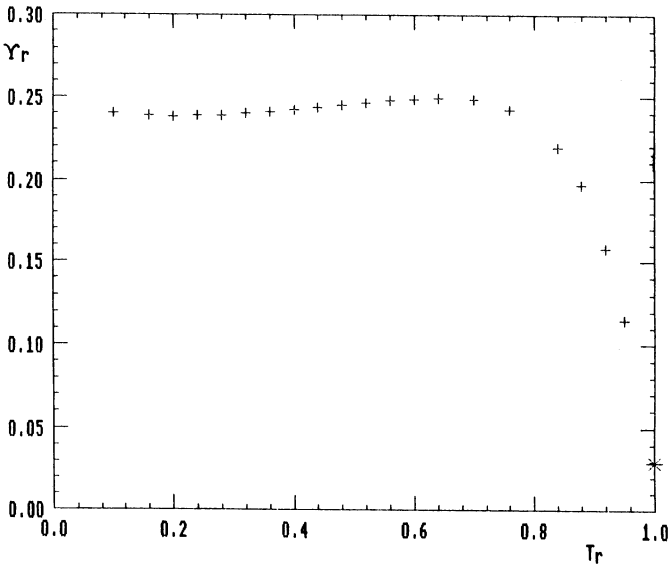

Fig. 14. As in Fig. 12, but with additional data points from the spline fit in Fig. 13. $C = 1.2$

of course, almost zero. The spline fit is excellent ($C = 1.2$, rms $= 0.08\%$) and it allows us to generate $Y(T)$ over an infinitely wide range of temperatures. In this way we were able to augment the data set shown in Fig. 12 and replot as a type 1 transition in Fig. 14, which shows that very high temperatures must be reached before the data points turn towards the Bethe limit. This example clearly demonstrates the advantage of treating such a transition as type 4.

10. Detection of errors and data analysis

In this section we give a selection of examples which show how the OMEUPS program can be used to detect errors and how, in some cases, it is able to improve existing data which has been shown to be deficient.

10.1. Tabulation errors

We show how the method may be used of detect two different types of tabulation error.

Individual entries may be incorrect or misprinted. An apparent case of this occurs in the 11-state RMATRX calculation of the rate coefficient for excitation of He (Table 6 of Berrington et al. 1985b). A plot of Y_r for the $2^3S \rightarrow 2^3P$ transition is shown in Fig. 15, and one sees immediately that one of the data points (corresponding to $T = 20{,}000$) deviates from the general trend of the others. Dr. K. A. Berrington (1987, private communication) has informed us that the correct value of $q(2^3S \rightarrow 2^3P)$ at this temperature is $4.8\ 10^{-7}$ cm^3 s^{-1} (i.e. $Y_r = 32$). Although the program OMEUPS in its present form is not intended for the spline fitting of neutral target data, it can be used for visually checking the validity of such data, as this example shows.

Our second example is concerned with the Y data for Si^{+2} obtained by Baluja et al. (1980, 1981b) from a 12-state close coupling calculation with the RMATRX code, using the target wave functions of Baluja & Hibbert (1980) who give the relevant oscillator strengths and term energies. Unfortunately, some of the Y results are unreliable since the collision code contained a programming error (see Dufton & Kingston 1989). While our method for analysing data cannot explain the basic cause of these errors, it is of interest to demonstrate its capability for detecting them.

Consider the pair of type 1 transitions linking $3s3p\,^1P$ to the terms $3p^2\,^1D$ and $3s3d\,^1D$. After processing the data by UPSILON, we obtained Figs. 16 and 17, which suggest that the Y data sets for the two transitions have been inadvertently interchanged, since $y_{3,4}(T) \rightarrow y_{3,10}(1)$ and $y_{3,10}(T) \rightarrow y_{3,4}(1)$, where $y_{i,j}(T_r)$ denotes $Y_r(T_r)$ for the $i \rightarrow j$ transition, and the target terms are labelled by indices as in Baluja et al. (1981b).

Corrected results for Si^{+2} given by Dufton & Kingston (1989) have now confirmed this conclusion, although the numerical values are slightly altered.

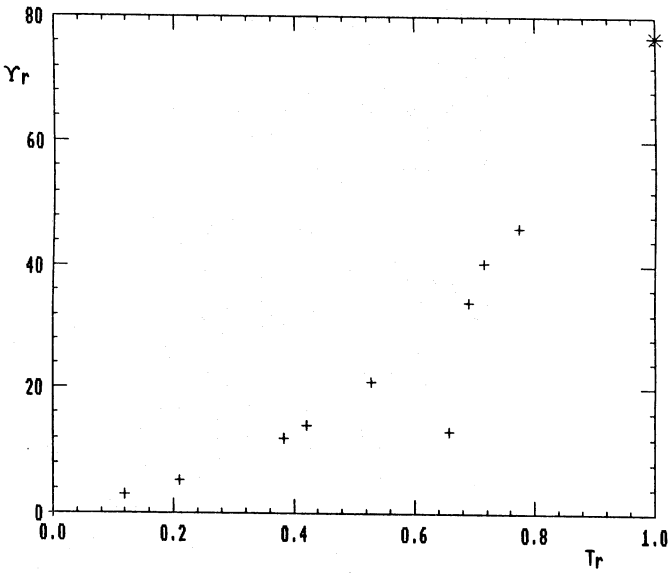

Fig. 15. He($1s2s\,^3S - 1s2p\,^3P$). Tabulation error detection; data from Berrington et al. (1985). $C = 1.45$

© European Southern Observatory • Provided by the NASA Astrophysics Data System

1992A&A...254..436B

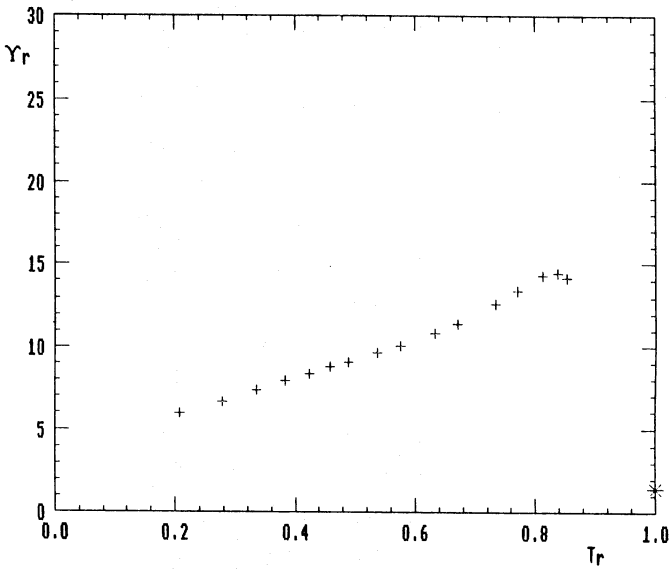

Fig. 16. $Si^{+2}(3s3p\,^1P - 3p^2\,^1D)$. Tabulation error detection; data from Baluja et al. (1981). $gf = 0.1242$ from Baluja & Hibbert (1980). $C = 1.3$

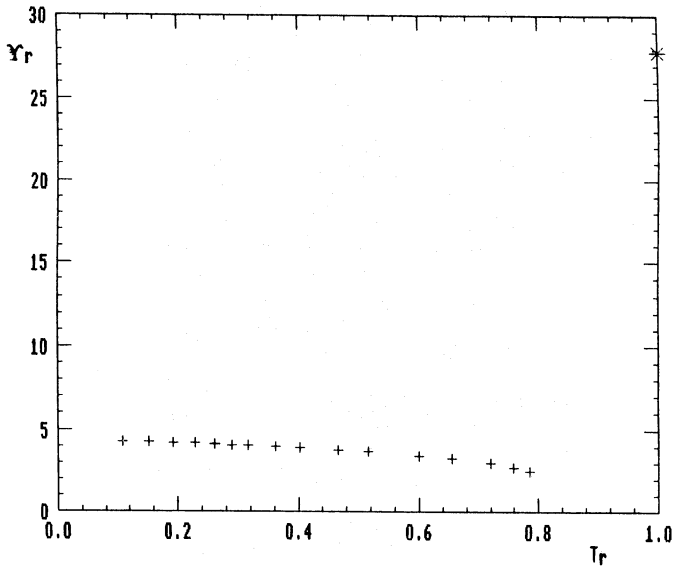

Fig. 17. $Si^{+2}(3s3p\,^1P - 3s3d\,^1D)$. Tabulation error detection; data from Baluja et al. (1981). $gf = 5.253$ from Baluja & Hibbert (1980). $C = 1.3$

It is interesting to note also that the data show signs of falling off at high temperatures due to omission of high angular momentum contributions; which effect is discussed in the next section.

10.2. Insufficient partial waves

Ω is obtained by summing partial collision strengths and sufficient of these should be included to ensure convergence. It is generally well known that, for type 1 transitions, distant encounters can make especially important contributions, which fortunately can be allowed for through the existence of a sum rule (Burgess 1974). However, for other transitions, many researchers truncate the expansion at an arbitrary value of L, which is independent of energy, and ignore the effect of higher partial waves altogether. This may result in Y being inaccurate at high temperatures owing to Ω falling off too fast with energy as $E \rightarrow \infty$.

As an example we show in Fig. 18 an optimised least squares spline fit to 16 data points of Baluja et al. (1981a) for the $2p^2\,^1D - 2p^2\,^1S$ transition in O^{+2}. The fit has an rms error of 0.56%, but does not tend to the Born limit 0.597 (see Tully & Baluja 1981) at $T_r = 1$, since the partial wave expansion was limited to $L \leqslant 3$. In Fig. 19 we have altered the 3rd, 4th and 5th knot values so that the spline no longer drops as $T_r \rightarrow 1$ but tends to the Born limit.

A second example is given in Fig. 20 where we plot Ω_r for the transition $3s^2\,^1S - 3s3d\,^1D$ in Fe^{+14}. The lower set of data points corresponds to the distorted wave calculation by Christensen et al. (1985) in which the partial wave expansion was summed up to $L = 11$. The data points do not tend to the Born limit 0.290 which we have calculated, and this suggests that the partial wave expansion has not converged. The lack of convergence was pointed out to Christensen et al. by J. B. Mann. A comment on this appears in their paper as a note added in proof, and the upper set of data points in Fig. 20 allows for the correction they give.

10.3. Invalid extrapolations

Most authors, when fitting Ω (or Y) data for type 1 transitions, use analytic expressions having the correct high energy (or temperature) functional form. However, sometimes the coefficient of the dominant logarithmic term is treated as one of the free parameters in the fitting, instead of ensuring that its value is correctly related to the gf value (see (8) and (26)). In this case, it is unlikely that any extrapolation of the fit will be valid.

As an example we consider the Y data of Pradhan et al. (1981b) for the $1s2s\,^1S - 1s2p\,^1P$ transition in Fe^{+24}, which they calculated by Maxwell integration of the Ω data of Pradhan et al. (1981a). Especially for the higher tabulated temperatures, some extrapolation of the Ω was needed in order to complete the integrations. Unfortunately, the coefficient of the logarithmic term was treated as a free parameter, and this resulted in its value being too large by a

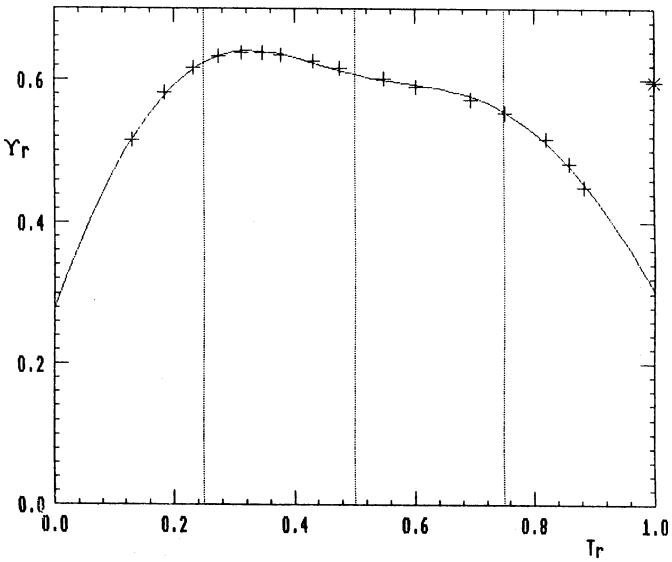

Fig. 18. $O^{+2}(2p^2\,^1D - 2p^2\,^1S)$. Insufficient partial waves in data from Baluja et al. (1981). * Born limit from Tully & Baluja (1981). $C = 1$

© European Southern Observatory • Provided by the NASA Astrophysics Data System

1992A&A...254..436B

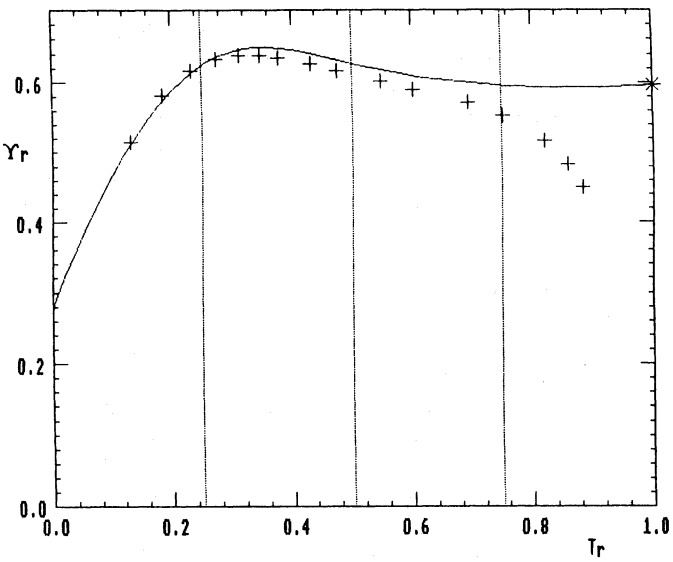

Fig. 19. As in Fig. 18, but with spline adjusted to allow for contribution from high angular momentum partial waves. $C = 1$ with knot values 0.2784, 0.6239, 0.6265, 0.5960, 0.5960

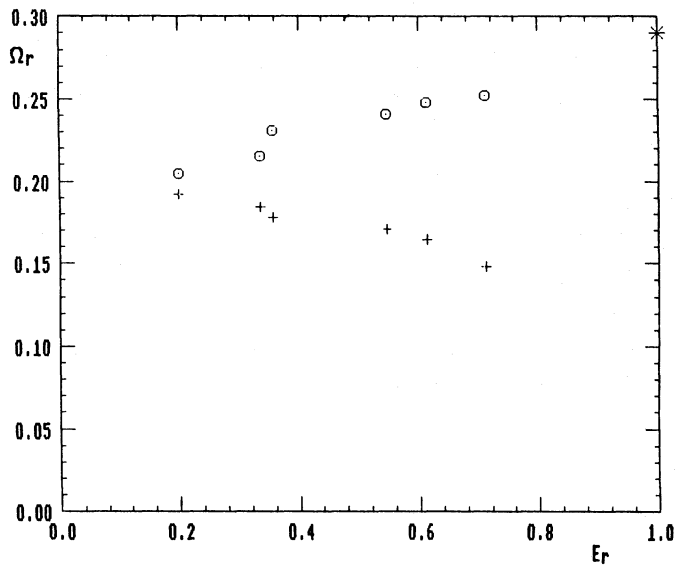

Fig. 20. $Fe^{+14}(3s^2\,{}^1S - 3s3d\,{}^1D)$. Showing the importance of high partial waves. Data from Christensen et al. (1985): + summation over $0 \leqslant L \leqslant 11$; ⊙ summation over $0 \leqslant L < 50$. * Born limit. $C = 5.2$

factor ~1.6. The effect of this is clearly shown in Fig. 21 where we plot $Y_r(T_r)$. The Y data of Pradhan et al. (1981b) for the corresponding transition in Be^{+2} and Ne^{+8} is similarly affected.

10.4. Data compacting

Results for $\Omega(E)$ and $Y(T)$ are usually presented in tabular form. Y, for example, is often given at several values of T spanning a region of arbitrary size centred on $T = T_m$ (see Sect. 8.2). There is no universally accepted way of laying out the table, and intervals in T may be regular or irregular. By transforming from $Y(T)$ to $Y_r(T_r)$

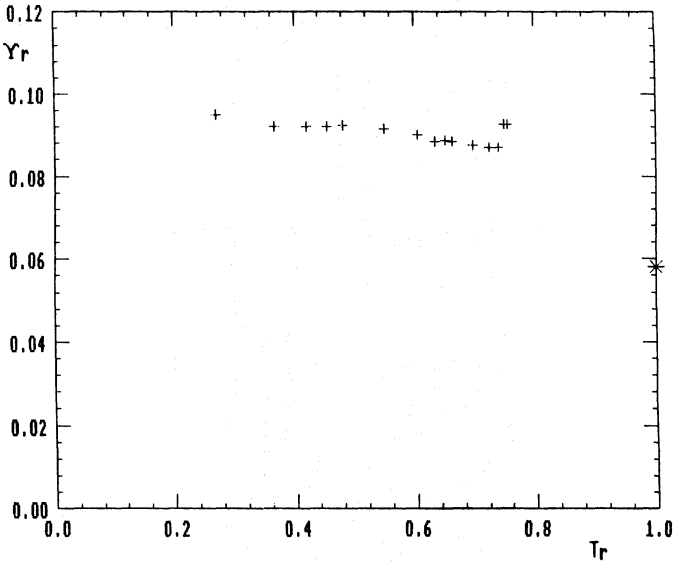

Fig. 21. $Fe^{+24}(1s2s\,{}^1S - 1s2p\,{}^1P)$. Effect of using an unsatisfactory high energy extrapolation. Y_r data from Pradhan et al. (1981b), $gf = 0.020$ from Pradhan et al. (1981a). * Bethe limit. $C = 8$

one may show if the original tabulation is too sparse in some regions of T. Conversely it can often suffer from an overabundance of information.

We illustrate this with an example taken from Mohan & Le Dourneuf (1990) who use a constant tabulation step $\Delta T = 5\ 10^4$ to span $10^5 \leqslant T \leqslant 10^6$. The transition we consider is $2p^5\,{}^2P - 2p^4({}^3P)3p\,{}^2D$ in Si^{+5}. Figure 22 underlines the point we are making, for more than half of the 19 data points are clustered into a small region on the rhs of the graph where the variation is almost linear. In this case it would have been preferable to use a constant step in log (T), say 0.1, thereby economizing 8 data points. Our procedure is even more economical since only 6 numbers are needed to reproduce the entire data set *and* extrapolate it to $T = 0$ and $T = \infty$.

We have calculated the high temperature limit (0.063) with the Born approximation and this is shown in Fig. 22. Mohan & Le Dourneuf's data points are in excellent agreement with the Born limit even though they truncated the partial wave expansion at $L = 12$. The optimised spline fit ($C = 0.19$, rms = 0.10%) is shown in Fig. 22.

10.5. Data comparison

Three independent calculations of the collision strength Ω for the $3s^2\,{}^1S - 3s3d\,{}^1D$ transition in S^{+4} have been reported; Feldman et al. (1981), Dufton & Kingston (1984), and Christensen et al. (1986). The published results are compared in Fig. 23, where we also give our spline fit to Christensen et al. The latter gave only 3 of their 6 calculated data points; however, further information about the full data set may be inferred, since Pradhan (1988) used an analytical fit to it in order to calculate Y. We therefore chose our spline fit to Ω so as to yield Y values in good agreement with those tabulated by Pradhan, while also fitting to the 3 values of Ω given in Christensen et al.; overall agreement to within ~2% was achieved.

Using the Born approximation and wave functions similar to those of Dufton & Kingston (1984), we obtain the high energy limiting value $\Omega_r(1) = 1.3$. As shown in Fig. 23, this is slightly higher than the Pradhan (1988) limiting value.

© European Southern Observatory • Provided by the NASA Astrophysics Data System

1992A&A...254..436B

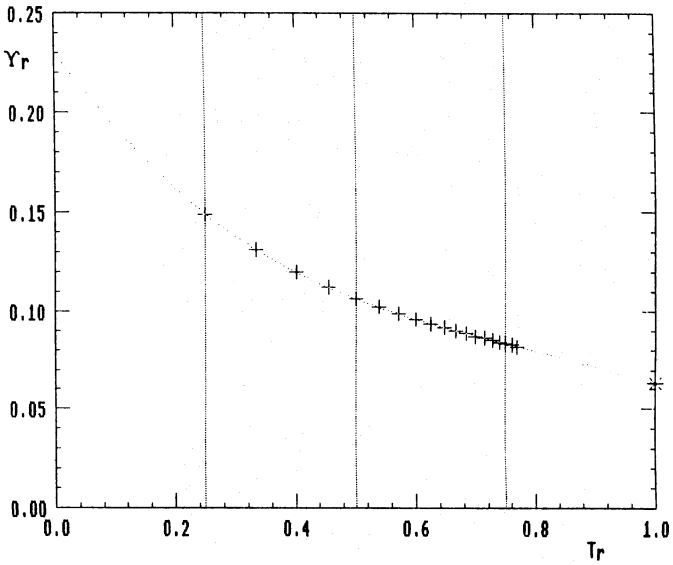

Fig. 22. $Si^{+5}(2p^5\,{}^2P - 2p^4 3p\,{}^2D)$. Compacting data from Mohan & Le Dourneuf (1990). * Born limit. $C = 0.19$ with knot values 0.2304, 0.1490, 0.1062, 0.08325, 0.06346

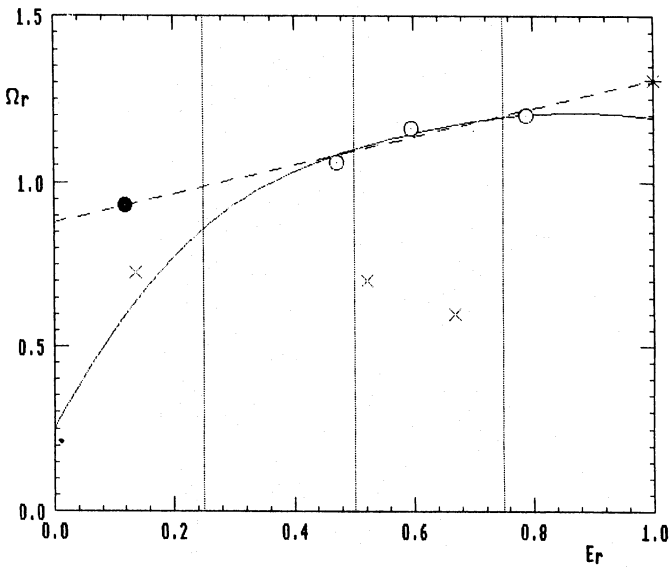

Fig. 23. $S^{+4}(3s^2\,{}^1S - 3s3d\,{}^1D)$. Comparison of data:
• Dufton & Kingston (1984); × Feldman et al. (1981); ⊙ Christensen et al. (1986). * Born limit. — spline fit to Christensen et al.

Feldman et al. (1981) retained partial waves only up to $L = 6$, which explains why their collision strength (calculated in a distorted wave approximation) falls off with increasing energy. Christensen et al. (1986) also used a distorted wave approximation but, in contrast to Feldman et al. (1981), they evaluated the contribution from all partial waves up to $L \sim 50$. It is therefore puzzling that their low energy results apparently lie below those of Feldman et al., and they lie even further below the point given by Dufton & Kingston.

On this evidence, a linear fit to the latter point and the $\Omega_r(1)$ Born limit point is probably as good a representation of $\Omega_r(E_r)$ as any, particularly since this also gives a reasonable fit to the 3 original data points given in Christensen et al., as is shown in Fig. 23. We therefore adopted this, to obtain the following spline fit to Y_r for this transition: $C = 2.4$ with knot values 0.8823, 1.014, 1.102, 1.185, 1.306.

11. Adaptation of the method for very strong resonances

Resonances make large rapidly varying contributions to Ω for many transitions, but the resulting thermally averaged Y can usually be handled satisfactorily by our method, as examples above show. However, one occasionally encounters a case where the effect of a bunch of resonances is so large that our usual 5-point spline fit to Y_r gives insufficient accuracy. In such cases, one can split the temperature range into two or more intervals and make separate 5-point fits for each interval, and our final example illustrates this.

We consider the type 2 transition $2p^5\,{}^2P_{3/2} - 2p^5\,{}^2P_{1/2}$ in Ni^{+19}, using collision data from Mohan et al. (1990), shown in Fig. 24. Large resonance contributions cause the bump near $\log T \approx 4.7$. Accurate fits can be made by dividing the entire range of T into two intervals.

Figure 25 shows the data corresponding to $0 \leqslant T \leqslant 10^6$ (including a value $Y = 0.042$ at $T = 0$ estimated from Fig. 1 of Mohan et al.), and our optimised 5-point spline fit for this interval. With $C = 0.18$ and knot values 0.04197, 0.05557, 0.1027, 0.09552, 0.07339, this gives an rms error of 0.59%.

The data points for $T \geqslant 10^6$ are shown in Fig. 26, with the high temperature limit value 0.0157 taken from Tully (1986). For this interval, the optimum fit ($C = 21$ and knot values 0.07455, 0.07661, 0.06778, 0.03791, 0.01570) gives an rms error of 0.19%.

For astrophysical applications, it should be noted that at $T = 10^6$ the ionization balance population of Ni^{+19} is a factor $\sim 10^{-22}$ below its maximum value (which occurs at $T \sim 6\ 10^6$). Hence, if the ionization is maintained by electron collisions (e.g. coronal type plasmas) only the second of these fits is needed. However, if the ionization is maintained by non-local high energy photons (e.g. nebular plasmas) the first fit may be required.

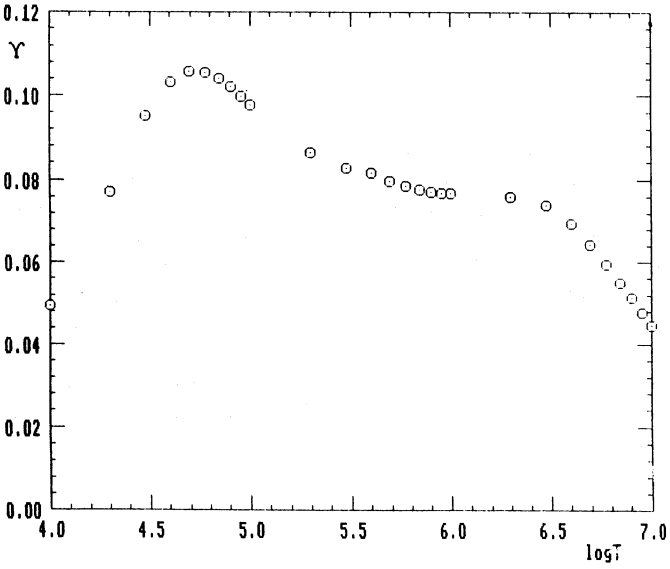

Fig. 24. $Ni^{+19}(2^2P_{3/2} - 2^2P_{1/2})$. Y data from Mohan et al. (1990)

© European Southern Observatory • Provided by the NASA Astrophysics Data System

1992A&A...254..436B

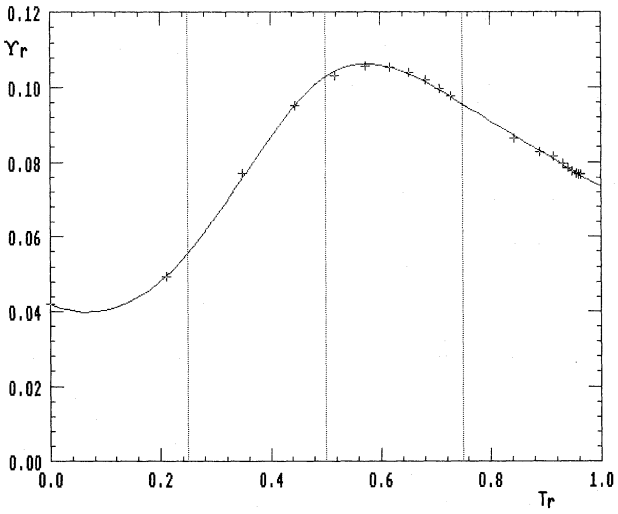

Fig. 25. $Ni^{+19}(2^2P_{3/2} - 2^2P_{1/2})$. Fit to Y_r data for $0 \leqslant T \leqslant 10^6$

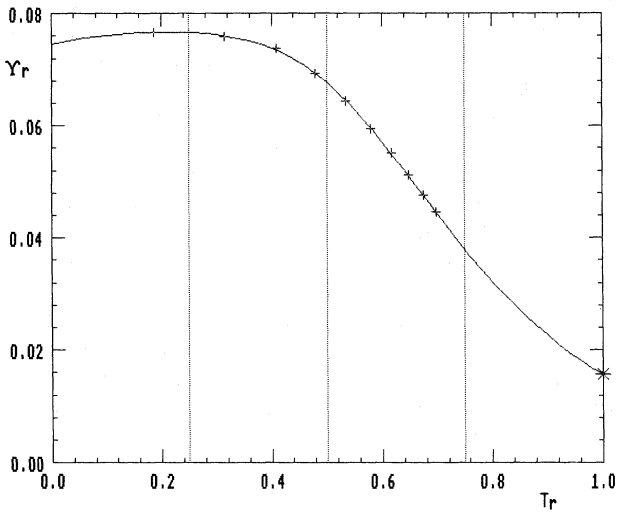

Fig. 26. $Ni^{+19}(2^2P_{3/2} - 2^2P_{1/2})$. Fit to Y_r data for $T \geqslant 10^6$

Acknowledgements. We are indebted to Jeff Payne for helping to implement the first BASIC version of our method on a Hewlett Packard System 45. Jim Lang and Peter McWhirter were salutary in the early stages as "caviae porcelli" when developing this first C-plot program. The more recent version dubbed OMEUPS has benefitted from assiduous testing to destruction by Marita Chidichimo and Helen Mason. We wish to thank Mike Seaton for his valuable comments on the manuscript, and Keith Berrington, custodian of the atomic data bank in Belfast, who was our turnkey and good-humoured guide to that wealthy and indispensable storeroom of collision strengths.

Appendix

Here we define our 5-point spline function, by means of a FORTRAN listing, and give other FORTRAN functions which may be of help in using our method.

```
      FUNCTION SPLINE(P1,P2,P3,P4,P5,X)
C 5-point spline interpolation of Y(X), for X in the range (0,1).
C Input:
C   Knot values P1=Y(0), P2=Y(1/4), P3=Y(1/2), P4=Y(3/4), P5=Y(1)
C   and X.
C Output:
C   SPLINE=Y(X).
C Code:
      S=1.0/30.0
      S2=32.0*S*(19.0*P1-43.0*P2+30.0*P3-7.0*P4+P5)
      S3=160.0*S*(-P1+7.0*P2-12.0*P3+7.0*P4-P5)
      S4=32.0*S*(P1-7.0*P2+30.0*P3-43.0*P4+19.0*P5)
      IF(X.GT.0.25) GO TO 1
      X0=X-0.125
      T3=0.0
      T2=0.5*S2
      T1=4.0*(P2-P1)
      T0=0.5*(P1+P2)-0.015625*T2
      GO TO 4
    1 IF(X.GT.0.5) GO TO 2
      X0=X-0.375
      T3=20.0*S*(S3-S2)
      T2=0.25*(S2+S3)
      T1=4.0*(P3-P2)-0.015625*T3
      T0=0.5*(P2+P3)-0.015625*T2
      GO TO 4
    2 IF(X.GT.0.75) GO TO 3
      X0=X-0.625
      T3=20.0*S*(S4-S3)
      T2=0.25*(S3+S4)
      T1=4.0*(P4-P3)-0.015625*T3
      T0=0.5*(P3+P4)-0.015625*T2
      GO TO 4
    3 X0=X-0.875
      T3=0.0
      T2=0.5*S4
      T1=4.0*(P5-P4)
      T0=0.5*(P4+P5)-0.015625*T2
    4 SPLINE=T0+X0*(T1+X0*(T2+X0*T3))
      RETURN
     END
```

```
      FUNCTION OMEGA(K,EIJ,C,P1,P2,P3,P4,P5,EJ)
C Collision strength, Omega.
C Input:
C   K=transition type,
C   EIJ=transition energy (Ryd.),
C   C=abscissa scale parameter,
C   P1,P2,P3,P4,P5=spline knot values,
C   EJ=colliding electron energy after excitation (Ryd.).
C Output:
C   OMEGA=Omega.
C Code:
      E=ABS(EJ/EIJ)
      IF ((K.EQ.1).OR.(K.EQ.4)) X=LOG((E+C)/C)/LOG(E+C)
      IF ((K.EQ.2).OR.(K.EQ.3)) X=E/(E+C)
      Y=SPLINE(P1,P2,P3,P4,P5,X)
      IF (K.EQ.1) Y=Y*LOG(E+2.71828)
      IF (K.EQ.3) Y=Y/((E+1)*(E+1))
      IF (K.EQ.4) Y=Y*LOG(E+C)
      OMEGA=Y
      RETURN
     END
```

```
      FUNCTION UPSIL(K,EIJ,C,P1,P2,P3,P4,P5,T)
C Maxwell averaged collision strength, Upsilon.
C Input:
C   K=transition type,
C   EIJ=transition energy (Ryd.),
C   C=abscissa scale parameter,
C   P1,P2,P3,P4,P5=spline knot values,
C   T=electron temperature (Kelvin).
C Output:
C   UPSIL=Upsilon.
C Code:
      E=ABS(T/(1.57888E5*EIJ))
      IF ((K.EQ.1).OR.(K.EQ.4)) X=LOG((E+C)/C)/LOG(E+C)
      IF ((K.EQ.2).OR.(K.EQ.3)) X=E/(E+C)
      Y=SPLINE(P1,P2,P3,P4,P5,X)
      IF (K.EQ.1) Y=Y*LOG(E+2.71828)
      IF (K.EQ.3) Y=Y/(E+1)
      IF (K.EQ.4) Y=Y*LOG(E+C)
      UPSIL=Y
      RETURN
     END
```

© European Southern Observatory • Provided by the NASA Astrophysics Data System

1992A&A...254..436B


```
      FUNCTION RATE(K,EIJ,WI,C,P1,P2,P3,P4,P5,T)
C  Rate coeff. for excitation or de-excitation by electron impact.
C  Input:
C    K=transition type,
C    EIJ=transition energy (Ryd.), (+ve for exc., -ve for de-exc.)
C    WI=initial statistical weight,
C    C=abscissa scale parameter (from Upsilon fit),
C    P1,P2,P3,P4,P5=spline knot values (from Upsilon fit),
C    T=electron temperature (Kelvin).
C  Output:
C    RATE=rate coefficient (cm**3/sec).
C  Code:
      R=1
      IF (EIJ.LE.0.0) GO TO 1
      R=0
      IF (T.GE.1000.0*EIJ) R=EXP(-EIJ*1.57888E5/T)
    1 S=1E70
      IF (T.GE.1E-70) S=SQRT(1.57888E5/T)
      U=UPSIL(K,EIJ,C,P1,P2,P3,P4,P5,T)
      RATE=2.1716E-8*S*R*U/WI
      RETURN
     END
```

References

Abramowitz M., Stegun I. A., 1965, Handbook of Mathematical Functions, NBS

Aller L. H., Menzel D. H., 1945, ApJ 102, 239

Baluja K. L., Hibbert A., 1980, J. Phys. B 13, L327

Baluja K. L., Burke P. G., Kingston A. E., 1980, J. Phys. B 13, L543

Baluja K. L., Burke P. G., Kingston A. E., 1981a, J. Phys. B 14, 119

Baluja K. L., Burke P. G., Kingston A. E., 1981b, J. Phys. B 14, 1333

Berrington K. A., Burke P. G., Dufton P. L., Kingston A. E., 1981, At. Data Nucl. Data Tables. 26, 1

Berrington K. A., Burke P. G., Dufton P. L., Kingston A. E., 1985a, At. Data Nucl. Data Tables. 33, 195 and 345 (erratum)

Berrington K. A., Burke P. G., Freitas L. C. G., Kingston A. E., 1985b, J. Phys. B 18, 4135

Berrington K. A., Burke P. G., Le Dourneuf M., Robb W. D., Taylor K. T., Vo Ky Lan, 1978, Comput. Phys. Commun. 14, 367

Bohm D., Aller L. H., 1947, ApJ 105, 1

Burgess A., 1992 (submitted)

Burgess A., Tully J. A., 1978, J. Phys. B 11, 4271

Burgess A., 1974, J. Phys. B 7, L364

Burgess A., Hummer D. G., Tully J. A., 1970, Phil. Trans. Roy. Soc. A 266, 225

Burgess A., Mason H. E., Tully J. A., 1988, J. Phys. (Paris) 49, C1–107

Burgess A., Mason H. E., Tully J. A., 1989, A&A 217, 319

Christensen R. B., Norcross D. W., Pradhan A. K., 1985, Phys. Rev. A 32, 93

Christensen R. B., Norcross D. W., Pradhan A. K., 1986, Phys. Rev. A 34, 4704

Clark R. E. H., Magee N. H. Jr., Mann J. B., Merts A. L., 1982, ApJ 254, 412

Cochrane D. M., McWhirter R. W. P., 1983, Phys. Scr. 28, 25

Dufton P. L., Hibbert A., Kingston A. E., Doschek G. A., 1983, ApJ 274, 420

Dufton P. L., Kingston A. E., 1984, J. Phys. B 17, 3321

Dufton P. L., Kingston A. E., 1989, MNRAS 241, 209

Feldman U., Doschek G. A., Bhatia A. K., 1981, ApJ 250, 799

Gaetz T. J., Salpeter E. E., 1983, ApJS 52, 155

Gallagher J. W., Pradhan A. K., 1985, JILA Report No. 30

Goldstein L., 1933, Ann. Phys. (Paris) 19, 305

Hayes M. A., Norcross D. W., Mann J. B., Robb W. D., 1977, J. Phys. B 10, L429

Hebb M. H., Menzel D. H., 1940, ApJ 92, 408

Ho Y. K., Henry R. J. W., 1983, ApJ 264, 733

Jordan C., 1969, MNRAS 142, 501

Keenan F. P., Berrington K. A., Burke P. G., Dufton P. L., Kingston A. E., 1986, Phys. Scr. 34, 216

Ljepojevic N. N., Burgess A., 1990, Proc. Roy. Soc. A 428, 71

Merts A. L., Mann J. B., Robb W. D., Magee N. H. Jr., 1980, Los Alamos Report LA-8267-MS

Mewe R., 1972, A&A 20, 215

Mohan M., Le Dourneuf M., 1990, A&A 227, 285

Mohan M., Le Dourneuf M., Hibbert A., Burke P. G., 1990, MNRAS 243, 372

Pradhan A. K., 1988, At. Data Nucl. Data Tables 40, 335

Pradhan A. K., Norcross D. W., Hummer D. G., 1981a, Phys. Rev. A 23, 619

Pradhan A. K., Norcross D. W., Hummer D. G., 1981b, ApJ 246, 1031

Sampson D. H., Goett S. J., Clark R. E. H., 1983, At. Data Nucl. Data Tables 29, 467

Seaton M. J., 1953, Proc. Roy. Soc. A 218, 400

Seaton M. J., 1955, Proc. Roy. Soc. A 231, 37

Tayal S. S., Kingston A. E., 1984, J. Phys. B 17, 1383

Tully J. A., 1978, J. Phys. B 11, 2923

Tully J. A., 1980, J. Phys. B 13, 3023

Tully J. A., Baluja K. L., 1981, J. Phys. B 14, L831

Tully J. A., 1986, IIème Colloque sur la Physique des Collisions Atomiques et Electroniques, Metz 18–20 juin

Zhang H. L., Sampson D. H., Fontes C. J., 1990, At. Data Nucl. Data Tables 44, 31

© European Southern Observatory • Provided by the NASA Astrophysics Data System